5-2017

Mechanical Performance of Natural / Natural Fiber Reinforced Hybrid Composite Materials Using Finite Element Method Based Micromechanics and Experiments

Muhammad Ziaur Rahman
Utah State University

MECHANICAL PERFORMANCE OF NATURAL / NATURAL FIBER REINFORCED HYBRID COMPOSITE MATERIALS USING FINITE ELEMENT METHOD BASED MICROMECHANICS AND EXPERIMENTS

by

Muhammad Ziaur Rahman

A thesis submitted in partial fulfillment
of the requirements for the degree

of

MASTER OF SCIENCE

in

Mechanical Engineering

Approved:

Thomas H. Fronk, Ph.D. Major Professor	Nick Roberts, Ph.D. Committee Member
Ling Liu, Ph.D. Committee Member	Mark R. McLellan, Ph.D. Vice President for Research and Dean of the School of Graduate Studies

UTAH STATE UNIVERSITY
Logan, Utah

2017

ABSTRACT

Mechanical Performance of Natural / Natural Fiber Reinforced Hybrid Composite Materials Using Finite Element Method Based Micromechanics and Experiments

by

Muhammad Ziaur Rahman, Master of Science

Utah State University, 2017

Major Professor: Thomas H. Fronk, Ph.D.
Department: Mechanical and Aerospace Engineering

A micromechanical analysis of the representative volume element (RVE) of a unidirectional flax/jute fiber reinforced epoxy composite is performed using finite element analysis (FEA). To do so, first effective mechanical properties of flax fiber and jute fiber are evaluated numerically and then used in evaluating the effective properties of flax/jute/epoxy hybrid composite. Mechanics of Structure Genome (MSG), a new homogenization tool developed in Purdue University, is used to calculate the homogenized effective properties. Numerical results are compared with analytical solution based on rule of mixture, Halpin-Tsai as well as Tsai-Hahn equations. The effect of the volume fraction of the two different fibers is studied. Mechanical performance of hybrid composite is compared with the mechanical performance of single fiber composites. Synergistic effect due to hybridization is studied using analytical method given in literature, finite element method based MSG and Classical Lamination Theory (CLT). It is found that, when Poisson ratio is taken into consideration, elastic modulus shows synergy due to hybridization. Finally, impact properties of flax/jute/epoxy hybrid composite material are studied using Charpy impact testing.

(107 pages)

PUBLIC ABSTRACT

Mechanical Performance of Natural / Natural Fiber Reinforced Hybrid Composite Materials Using Finite Element Method Based Micromechanics and Experiments

Muhammad Ziaur Rahman

A micromechanical analysis of the representative volume element (RVE) of a unidirectional flax/jute fiber reinforced epoxy composite is performed using finite element analysis (FEA). To do so, first effective mechanical properties of flax fiber and jute fiber are evaluated numerically and then used in evaluating the effective properties of flax/jute/epoxy hybrid composite. Mechanics of Structure Genome (MSG), a new homogenization tool developed in Purdue University, is used to calculate the homogenized effective properties. Numerical results are compared with analytical solution based on rule of mixture, Halpin-Tsai as well as Tsai-Hahn equations. The effect of the volume fraction of the two different fibers is studied. Mechanical performance of hybrid composite is compared with the mechanical performance of single fiber composites. Synergistic effect due to hybridization is studied using analytical method given in literature, finite element method based MSG and Classical Lamination Theory (CLT). It is found that, when Poisson ratio is taken into consideration, the longitudinal and transverse elastic moduli can show synergy due to hybridization. Finally, impact properties of flax/jute/epoxy hybrid composite material are studied using Charpy impact testing.

To my parents Joinab and late Kamalur, to my siblings, and finally to all my teachers

ACKNOWLEDGMENTS

I would like to express my sincere gratitude to my advisor Dr. Thomas H. Fronk for the continuous support of my research work, for his patience, motivation, enthusiasm and immense knowledge. His supervision helped me in all the time of research and writing of this thesis. I could not have imagined having a better advisor and mentor for my MS study.

Also, I would like to thank the rest of my thesis committee: Dr. Nick Roberts, and Dr. Ling Liu, for their encouragement and insightful comments. My appreciation also goes to the staff of the MAE department, Chris Spall, Karen Zobell and Terry Zollinger, who helped during the course of my study.

I thank my fellow lab mate Mohammed for all the support during numerical modeling and experimentation. Also I thank my friends Mehedi Hasan and Asaduzzaman Towfiq for their continuous support and motivation. I thank the Bangladesh community here at Utah State University, for their help at times.

Finally, my gratitude to my parents, siblings, and all my teachers, without whom I couldn't come to the point I am now. Special thanks to my teacher from high school Mr. Enamul Haque.

Muhammad Ziaur Rahman

CONTENTS

LIST OF TABLES

LIST OF FIGURES

Figure Page

ACRONYMS

FEA	Finite Element Analysis
RVE	Representative Volume Element
PBC	Periodic Boundary Conditions
SEM	Scanning Electron Microscopy
RoHM	Rule of Hybrid Mixture
MSG	Mechanics of Structure Genome
DNS	Direct Numerical Simulation
DOF	Degrees of Freedom
UC	Unit Cell

CHAPTER 1
INTRODUCTION

1.1 Motivation

Environmental concerns related to the use of synthetic fiber reinforced polymer matrix composites have propelled the development of composite materials based on natural or renewable sources [3, 4]. Bio composites composed of natural fibers in synthetic or natural polymer matrices have recently gained much attention due to their low cost, environmental friendliness and their potential to compete with synthetic composites [5–8]. Natural fiber reinforced polymer composites have been used for many application such as automotive components, aerospace parts, sporting goods and building industry. In recent years, natural fibers have found increased application in bridge and building construction. In addition, some other factors behind the increased popularity of the natural fibers are low self-weight, high specific strength, free formability and substantial resistance to corrosion and fatigue [9]. Nonetheless, the use of natural composites has been limited due to their lower mechanical and thermo-physical properties compared to synthetic composites and conventional structural materials [8].

The word hybrid is of Greek-Latin origin and can be found in numerous scientific fields. In the case of polymer composites, hybrid composites are these systems in which one kind of reinforcing material is incorporated in a mixture of different matrices (blends) [10] or two or more reinforcing and filling materials are present in a single matrix [11]. The incorporation of two or more natural fibers into a single matrix has led to development of hybrid composites. The behavior of hybrid composites is a weighed sum of the individual components in which there is more favorable balance between the inherent advantages and disadvantages. While using a hybrid composite that contains two or more types of fiber, the advantages of one type of fiber could complement with what are lacking in the other [9]. As

a consequence, a balance in cost and performance could be achieved through proper material design [12]. The strength of the hybrid composites is dependent on the properties of fiber, the aspect ratio of fiber content, length of individual fiber, orientation of fiber, extent of intermingling of fibers, fiber to matrix interface bonding and arrangement of both the fibers and also on failure strain of individual fibers. Maximum hybrid results are obtained when the fibers are highly strain compatible [13].

Polymer composites with hybrid reinforcement solely constituted of natural fibers are less common, but these are also potentially useful materials with respect to the environmental concerns. Natural fiber reinforced composites are initially aimed at the replacement of glass fiber reinforced composites [14]. Depending on the exact nature of fiber needed, lignocellulosic fibers (natural fibers) are in most cases cheaper than glass fibers. Lignocellulosic fibers are also expected to cause less health problems for the people producing the composites compared to glass fiber based composites. Lignocellulosic fibers do not cause skin irritations, itching and they are not suspected of causing lung cancer, like they do for the case of very small glass fibers [9]. Among natural fibers, flax is known to produce a large amount of dust. But this problem exists in the early stages of the flax fiber isolation process. More importantly, this is fairly well under control in the modern flax processing industries . Another positive aspect of natural fibers is that they have a lower density and lower specific weight compared to glass fibers. So a hybrid with, for example, kenaf/flax will be lighter than a hybrid with kenaf/glass.

Although there are some literature available involving natural/natural fiber reinforced composites, most of the time they are based on experiments only. Some of these works could be found in references [15–19]. But doing an experiment is sometimes costly and time consuming. On the other hand numerical simulation using FEA is cost effective. In addition, the fiber-matrix combination can easily be changed to see the fiber matrix interaction. The volume fraction of the fibers can also be changed easily. For all these reasons, numerical simulation is, sometimes, a better alternative compared to experiments, specially to use a variety of combination of fibers and matrices along with a varying volume fractions of

fibers. But it does not mean that the importance of experiment can totally be denied. After designing a successful finite element model, it is necessary to develop it practically in the laboratory to check if it is showing the expected response or not. Sometimes experiments are required to validate the numerical results. And sometimes experiments are the only solution to finding out material properties to be used in numerical simulation. That's why we are interested in doing the micromechanics modeling of natural/natural fiber reinforced hybrid composites to find out the elastic constants and the mechanical properties of the hybrid material. Here we have used flax/jute reinforced epoxy composite material. We also have carried out Charpy impact testing of the flax/jute/epoxy hybrid composite material to study the impact behavior of it.

1.2 Why Hybridization

Due to the cost of graphite, researchers and industrialists came up with a novel idea of incorporating glass into the same matrix containing graphite. The idea is that some of the graphite fibers would be replaced by glass fibers which would reduce the cost of the composite material. At the same time the superiority in mechanical performance would also not be hindered to a large extent because of the presence of graphite fibers in the same matrix. This idea resulted in graphite/glass hybrid composite. Next, due to environmental concern and also with a hope of reducing the cost even more, scientists started to think of replacing graphite from graphite/glass hybrid composite by some kind of natural fibers. In this way, the cost of the composite material would reduce even more due to the abundance of natural fibers while the mechanical performance of newly formed glass/natural fiber reinforced composite would not be hindered significantly. Then due to environmental concern, scientists considered using only natural fiber reinforced composite. The pros of using natural fiber reinforced composite is that it would become recyclable, the cost would be less and it would be free from any blame of causing lung cancer of the workers involved in composite manufacture like the short glass fibers do. But the problem of natural fiber is that, a single type of natural fiber does not possess all necessary mechanical properties i.e. tensile strength, flexural strength, impact strength, elongation at break etc. so that

the performance of the composite would be competitive. Some of the natural fibers show superior tensile and flexural strength, but are weak in impact strength and elongation at break. Some of them are superior at impact strength and elongation at break, but have weak performance in tensile and flexural strength. That is why the researchers considered using two (or even more) types of natural fiber in the same resin. This is called natural/natural fiber reinforced hybrid composite. In this way, the limitation of one type of fiber could successfully be overcome by the second type of fiber.

1.3 Basic Assumption of Failure

In the section 1.4, a detailed description of the work available in literature has been presented. In all the works it is assumed that there is a perfect bonding existent in between the fiber and the matrix. That means the failure would not be due to fiber pull out from the matrix. Most of the papers have ignored the effect of delamination. In all the works, it is assumed that in the fiber direction, the failure will initiate due to the failure of matrix. In the transverse direction which is perpendicular to the fiber direction, the failure may occur in fiber instead of matrix.

1.4 Literature Review

Many researchers [20,21] & (C. C. Eng, N. A. Ibrahim, N. Zainuddin, H.Ariffin, W. M. Z. W. Yunus, 2014) have studied the suitability, competitiveness and capabilities of natural fibers embedded in polymeric matrices. They have also tried hybridization of natural fiber with a second natural or a synthetic fiber. Whether a hybridization is efficient or not is determined from the positive and negative hybrid effect. A positive or negative hybrid effect is defined as a positive or negative deviation of a certain mechanical property from the rule of hybrid mixture. The term hybrid effect has been used to describe the phenomenon of an apparent synergistic improvement in the properties of a composite containing two or more types of fiber (F. R. Jones, 1994). The selection of the components that make up the hybrid composite is determined by the purpose of hybridization and requirements imposed on the material or the construction being designed. The problem of selecting the type of

compatible fibers and the level of their properties is of prime importance when designing and producing hybrid composites [12].

In terms of fibers, three types of hybridizations are possible, namely-

1. Synthetic/synthetic fiber reinforced resin
2. Natural/synthetic fiber reinforced resin
3. Natural/natural fiber reinforced resin

Regarding synthetic/synthetic fiber hybridization, carbon/glass combination is the most popular. Most recently, Banerjee et.al. have done micromechanical analysis of the RVE of E-glass/carbon fiber reinforced epoxy matrix composites [22]. The different hybrid laminates are prepared by using short carbon fibers and glass fibers which are used to reinforce epoxy. In their study, the elastic constant and strength properties have been evaluated by using analytical formula and the results are compared with the FEA results. Variability in mechanical properties due to different locations of the two fibers for the same volume fractions is studied. They have reported negligible variability in elastic constants and longitudinal strength properties. But the variability in the transverse strength properties is significant. There are numerous number of other works available in literature on carbon/glass reinforced composite materials, for example in [23, 24].

Among all other synthetic/natural fiber reinforced hybrid composites, the combination of glass with a natural fiber is the most popular. Glass has been used as a reinforcement with different natural fibers in different times. For example Davoodi et.al. reinforced epoxy resin with kenaf/glass combination(M. M. Davoodi, S. M. Sapuan, D. Ahmad, Aidy Ali, A. Khalina &Mehdi Jonoobi, 2010). They find that developed hybrid composite possesses similar mechanical properties like typical material except impact properties. They conclude that kenaf/glass hybrid may be utilized for making structural components of car. On the other hand Cicala et. al. has considered hybridization of glass fiber with hemp, kenaf and flax for applications in the piping industry(G. Cicala, G. Cristaldi, G. Recca, G. Ziegmann, A. El-Sabbagh & M. Dickert, 2009). The hybrid composite laminates have been tested after immersion in aqueous acid solutions for 40 days. The mechanical test shows only a small

variation of the mechanical properties after immersion. In a very recent work, Ramesh et. al. has used kenaf/glass hybrid composites and showed that mechanical properties of the hybrid are comparable with the pure synthetic fiber reinforced composites, which shows the potential for hybridization of kenaf fiber with glass(M. Ramesh & S. Nijanthan, 2016).

As said before, composites constituted of two types of natural fibers are less common, instead of their high potential for structural applications. Most of the works on natural/natural fiber reinforced composites are experimental works. Some of them could be found in [15–19].The type of natural fibers to be used as hybrid reinforcement highly depends on the purpose of the use of the composite material and also on the load type. As an exemplar, oil palm empty fruit branches (EFB) and jute can be used as hybrid reinforcement. The volume ratio of EFB to jute could be $4:1$ or $1:4$. It depends on the purpose of use of the hybrid material. If the purpose is to use it under high tensile and flexural loading, one might want to use $4:1$ ratio of jute to EFB. It's because the tensile and flexural strength of jute fibers are much more compared to EFB fibers. But if the purpose is to reduce the weight significantly, one might want to use $1:4$ volume ratio of jute to EFB. Mechanical performance of natural/natural fiber also depends on layering pattern and length of the fibers. Discussion regarding these is presented in the following paragraphs under respective literature review.

In a paper by Idicula et. al. [15] the authors have used banana/sisal hybrid composites. The reason behind using a hybrid composite instead of using single fiber composite is to integrate both the tensile strength and the impact strength in the same composite material. They have showed in their work that at 0.4 fiber volume fraction, with the increase of relative volume fraction of banana with respect to sisal, tensile strength increases. On the other hand, with the increase of relative volume fraction of sisal, impact strength increases. In general, the tensile strength of fiber increases with increasing cellulose content and decreasing spiral angle with respect to the fiber axis. As the cellulose content of banana and sisal fiber is almost the same, spiral angle of the microfibrils is the determining factor of tensile strength. The spiral angle of banana (11°) is smaller than that of sisal (20°). Hence the in-

herent tensile properties of banana is larger than that of sisal. That is why with the increase of relative volume fraction of banana, tensile strength increases. But this increase in tensile (and flexural) strength is compensated by a loss in impact strength. So the increase of tensile as well as impact strength is a kind of trade off, which is determined by the increase (or decrease) of relative volume fraction of banana and sisal. That's why an optimum ratio of banana to sisal volume is yet to be determined. The authors have also showed that in banana/sisal hybrid composite, the tensile and flexural strengths show positive hybrid effect while the impact strength shows a negative hybrid effect. To be precise, when the banana is 67 relative vol% , the tensile strength is found to be the maximum. With even more increase in the relative volume of banana, tensile strength slightly decreases. When the banana is 67 relative vol% in the hybrid composites, the increase in tensile strength compared to sisal/polyester composites is 17, 28, 12 and 17% at $0.20, 0.30, 0.40$ and 0.50 V_f (V_f=volume fraction of fiber with respect to matrix) respectively. Maximum flexural strength is found when banana to sisal volume ratio is $1:1$. When banana is 67 relative vol% (at which tensile strength is maximum), the flexural strength slightly reduces than that of 50 relative vol% of banana, still it is larger than sisal/polyester composite. Regarding impact strength, highest impact strength is found for $V_f = 0.5$. And clearly the impact strength is highest for a sisal/polyester composite (relative vol% of banana=0). Another important aspect of using a hybrid composite is that it makes a synergistic increase in elongation at break. For example, elongation at break of banana is $3-4\%$ whereas of sisal is $6-7\%$. Integrating both of them in the same matrix results in a synergistic increase of elongation at break.

In a recent work by Jawaid et. al. [19], the authors have used high strength jute fiber along with low strength oil palm EFB. Instead of lower flexural strength, the reason behind using EFB is due to its low weight and high impact strength. That means jute fiber will contribute towards the increase of strength property while EFB will contribute towards the increase of impact property and will reduce weight. The authors used pure EFB composite, EFB/jute/EFB pattern, jute/EFB/jute pattern and pure jute composite. They show that at $V_f = 0.4$, when volume ratio of EFB and jute is $4:1$,the jute/EFB/jute pattern shows

a superior flexural strength and the flexural modulus compared to the EFB/jute/EFB pattern. It is because jute has a higher flexural strength. So under bending load, where the top and bottom lamina experience the highest tensile and compressive stress, putting jute as a skin material and EFB as a core material yields in higher flexural strength and flexural modulus. They also point out that as jute reinforced composite has a higher flexural modulus than EFB reinforced composite, under same stress, jute reinforced lamina will deform more than EFB reinforced composite. So there is a possibility that delamination will occur. The authors have used sandwich theory, according to which jute/EFB/jute laminate can be considered as an I-beam, where the skin material (jute lamina) acts as an I-beam flange and the core material (EFB lamina) acts as the beams shear web. The skins are subjected to compression/tension and are largely responsible for the strength of the sandwich laminate. On the other hand the core material absorbs the shear stress generated by the local bending forces and distributes them over a larger surface area in the sandwich composite. Regarding impact strength, due to higher impact strength of EFB reinforced composite, an EFB/jute/EFB pattern yields in a higher impact strength compared to a jute/EFB/jute pattern.

Saw et. al. and co workers have hybridized epoxy with jute and coir (S. K. Saw, K. Akhtar, N. Yadav & A. K. Singh, 2014). The jute fiber has high cellulose content, high aspect ratio and smaller microfibril angel (8.1°) which result in high tensile strength. Coir has larger microfibril angle which results in smaller tensile strength. But coir has some other attractive properties like very low density ($1 - 1.2 g/cm^3$) compared to other natural fibers and high failure strain value ($40 - 45\%$). So by introducing coir into jute reinforced epoxy, the weight of the composite structure can be reduced and the failure strain can be increased. But at the same time, due to the introduction of a low strength fiber into the resin, the final tensile strength of the structure will be reduced to some extent. Saw et. al. has used pure jute, jute/coir/jute hybrid, coir/jute/coir hybrid and pure coir composites. They have found that tensile strength, tensile modulus and impact strength are maximum for a jute reinforced epoxy. But elongation at break for jute reinforced composite is very small

compared to coir reinforced composite. Thus by introducing coir in to matrix alongside the jute fibers, elongation at break can be increased significantly.

In a paper by Khanam et. al. (P. N. Khanam, M. M. Reddy, K. Raghu, K. John & S. V. Naidu,2007), sisal/silk reinforced unsaturated polyester matrix composite has been tested under three different fiber length conditions-1cm, 2cm and 3cm. They show that when the sisal and silk fiber lengths are 2cm, the composite structure shows superior tensile, flexural and compressive properties. Moreover, surface treatment of the fibers even more increases the mechanical properties. That means, the highest tensile, flexural and compressive strengths can be found for 2cm sisal/silk fibers treated by chemical agents.

In another article by Medeiros et.al., the authors reinforce phenolic composites by jute/cotton hybrid fabrics to find out the mechanical properties of the hybrid structure [25]. They find that the composite properties are strongly influenced by test direction and rovings/fabric characteristics. They also have found that jute promotes a higher reinforcing effect while cotton avoids catastrophic failure.

Jacob and co-workers, in a study used rubber composites reinforced with sisal/oil palm hybrid fibers [17]. They have tried to find out how the strength of the composite varies with the variation of fiber length and fiber loading (fiber volume fraction). They find that tensile strength, elongation at break and tensile modulus at 100% elongation of the composite are maximum when the length of sisal and oil fibers are 10mm and 6mm respectively. Regarding fiber loading, they have found that tensile strength increases up to 30phr (parts per hundred rubber), then it decreases.

Most of the papers mentioned above, have used thermoset hybrid composites. Although thermosets are non-recyclable, which is one of the desired properties of natural/natural hybrid composites, they still are lighter in weight compared to synthetic composites and also they are cheaper in price.

Finding out two different kinds of natural fibers compatible to each other to be used in the same polymer for reinforcement is the vital task for hybridization. There are few factors needed to be considered while choosing fiber combination for hybridization. They

are-

1. Volume fraction of low elongation (LE) fiber and high elongation (HE) fiber
2. Failure strain ratio for the two fibers
3. Stiffness of the HE fiber (Y. Swolfs, I. Verpoest, L. Gorbatikh, 2016).

The hybrid effect will be larger when the volume fraction of LE fiber is lower than 50% of the total fiber volume fraction. To get a positive hybrid effect, the failure strain ratio needs to be 2. That means ratio of the failure strain of HE fiber reinforced composite to failure strain of the LE fiber reinforced composites needs to be 2. A ratio even higher does not significantly increase the performance. Finally, the more the stiffness of the HE fiber, the more the hybrid effect is. In addition to this, Marom et.al. reported that to get a positive hybrid effect, the layers of the different reinforcements need to be more distinct and segregated [26].

In our project, we have used flax/jute/epoxy hybrid composite material. The motivation behind using flax is that it has superior mechanical properties compared to other natural fibers. Jute is chosen because it is cheap and is light in weight. Epoxy is chosen as a resin material because it is a thermoset polymer, and hence has a high melting temperature along with excellent surface energy. The thesis can be subdivided broadly in three sections, namely, calculation of effective properties of flax fibers & jute fibers and then calculating effective properties of flax/epoxy, jute/epoxy, flax/jute/epoxy; study of synergistic effect due to hybridization of two natural fibers in the same matrix material in details; study of impact strength of flax/jute/epoxy hybrid composite material using experiments.

1.5 Hypothesis

A pair of natural fibers compatible to each other embedded in a suitable resin will yield in a composite material which is environmentally friendly, recyclable and low weight with competitive mechanical properties.

1.6 Overview

The thesis is divided in to six chapters followed by references at the end. The chapters are as follows:

1. Introduction
2. Research Objectives
3. Approach
4. Effective Mechanical Properties of Flax/Jute/Epoxy Hybrid Composite
5. Synergistic Effect Due to Hybridization
6. Impact Properties of Flax/Jute/Epoxy Hybrid Composite

In the first chapter, discussion includes motivation behind this project, literature review and some conclusions from the literature. Chapter 2 includes the research objectives. Chapter 3 explains the approach used to achieve the objectives. Chapter 4 describes the numerical modeling procedure used in calculating effective properties. Effective properties of flax fiber, jute fiber, flax/epoxy, jute/epoxy and flax/jute/epoxy are also given in this chapter. Chapter 5 elaborates the possibility and extent of synergistic effect due to hybridization. Finally, chapter 6 provides insight of impact behavior of flax/epoxy, jute/epoxy and flax/jute/epoxy hybrid composite.

1.7 Properties of Natural Fibers

A table containing mechanical properties of commercially important natural fibers is given below (Table 1.1). The table is collected from reference [9] where the authors have gathered these properties from different sources. Readers are requested to check the reference [9] to look for those sources.

Table 1.1: Mechanical Properties of Natural Fibers

Fibers	Density (g/cm^3)	Tensile Strength (MPa)	Young Modulus (GPa)	Elongation at break (%)
OPEFB	0.7-1.55	248	3.2	2.5
Flax	1.4	800-1500	60-80	1.2-1.6
Hemp	1.48	550-900	70	1.6
Jute	1.46	400-800	10-30	1.8
Ramie	1.5	500	44	2
Coir	1.25	220	6	15-25
Sisal	1.33	600-700	38	2-3
Abaca	1.5	980	-	-
Cotton	1.51	400	12	3-10
Kenaf (bast)	1.2	295	-	2.7-6.9
Kenaf (core)	0.21	-	-	-
Bagasse	1.2	20-290	19.7-27.1	1.1
Henequen	1.4	430-580	-	3-4.7
Pineapple	1.5	170-1627	82	1-3
Banana	1.35	355	33.8	5.3

CHAPTER 2

RESEARCH OBJECTIVE

- Calculate the effective mechanical properties of flax fiber, jute fiber and flax/jute/epoxy hybrid composite material
- Study if synergistic effect due to hybridization exists and the extent of it
- Study the impact strength of flax/epoxy, jute/epoxy and flax/jute/epoxy hybrid composite material

CHAPTER 3

APPROACH

Based on the research objectives given in the previous chapter, the following tasks have been identified and proposed. The tasks can be divided into three sections, numerical modeling, analytical modeling, and experimentation.

Numerical Modeling

- Study the cross-section and surface morphology of flax fiber and jute fiber using scanning electron microscopy. This is necessary to determine the type of RVE (circular, square or hexagonal etc.) to be used to evaluate effective mechanical properties of flax and jute fibers.

- Evaluate the effective mechanical properties of flax fiber and jute fiber using finite element method based Mechanics of Structure Genome (MSG). It can be done in two steps.

  (a) Draw RVEs of cell wall layers and evaluate elastic properties of them

  (b) Draw RVEs of flax fiber cell and jute fiber cell consisting of cell wall layers and evaluate elastic properties of the fibers

- Draw RVEs of flax/epoxy, jute/epoxy and flax/jute/epoxy and find effective mechanical properties of them. Different combination of volume of flax and jute fiber will be used while the total fiber volume fraction will be kept fixed. The purpose of this study is to understand the effect of increasing one type of fiber in the hybrid composite material.

- Draw an RVE of a two-phase layered composite and study if synergistic effect exists and the extent of it. Among the two phases, one phase will represent flax/epoxy laminae, while the other phase will represent jute/epoxy laminae.

Analytical Modeling

- Analytical methods like rule of hybrid mixture (RoHM) and Halpin-Tsai equations will be used to find the mechanical performance of flax/jute/epoxy hybrid composite material. Analytical results will be compared with the numerical results.

Experimentation

- Charpy impact testing will be carried out to study the impact behavior of flax/epoxy, jute/epoxy and flax/jute/epoxy hybrid composite material.

CHAPTER 4
EFFECTIVE MECHANICAL PROPERTIES OF FLAX/JUTE/EPOXY HYBRID COMPOSITE

4.1 Introduction

This chapter presents numerical models of flax fiber, jute fiber and flax/jute/epoxy hybrid composite material to predict the effective properties of them. The finite element method was applied along with SWIFTCOMP as a homogenization tool to accomplish this objective. SWIFTCOMP, developed in Purdue University, uses mechanics of structure genome (MSG), a unified approach recently introduced for multiscale constitutive modeling. To predict the effective properties of unidirectional flax/jute/epoxy hybrid composite material, numerical homogenization was carried out in two steps. In the first step, effective properties of flax and jute fiber were calculated using MSG. In the second step effective properties of flax/jute/epoxy hybrid composite were calculated using MSG.

Composites by nature are anisotropic and heterogeneous. On the other hand, most of the conventional materials like aluminum and glass can safely be assumed to be isotropic and homogeneous. Anisotropy can be dealt with using coordinate transformation. One can easily transform the material properties measured in the material coordinates into the problem coordinates and thus get rid of the issue of anisotropy. Heterogeneity, in principle, can be dealt with by using direct numerical simulation (DNS) of the composite structure containing all the microstructural details using finite element analysis (FEA). But this requires an extremely fine mesh. Extremely fine mesh results in millions of degrees of freedom (DOF). In fact, for most of the realistic composite structures, trillions of DOFs are needed. Getting an access to hardware and software to carry out such a vast FEA is not always possible. As an exemplar, with a very fine FEA discretization, we need to have millions of DOFs in our FEA model to analyze even a very tiny $1mm^3$ material

block [27]. With properly constructed models, heterogeneous composites can be replaced with an effective homogeneous material to achieve almost the same accuracy as DNS. It will cost many orders of magnitude less, even though care should be taken at the places having significant changes in geometry, load conditions, material properties, or close to boundaries. The concept of replacing the original heterogeneous multi-phase model with a homogeneous model is called homogenization. Homogenization is applied on a representative block of the original heterogeneous material, which acts as a tiny point when compared to the whole structure. As a tiny microstructural representative block is used for homogenization purpose, the mechanics involved in it is called micromechanics. Homogenized models are imaginary, but equivalent to the original heterogeneous materials. Such a homogenization can be achieved using atomistic simulations or experiments.

The first aim of micromechanics is to theoretically predict the effective macroscopic properties of heterogeneous materials in terms of microstructure. To do that, the microstructure, which is representative of the original structure with geometry and constitutive relations of constituents of the original structure, is homogenized to get an imaginary homogeneous material. This step is called homogenization [Figure 4.1]. Homogenization can be used either for constitutive modeling, where the complete set of effective materials properties of three-dimensional (3D) structure can be deduced, or for simulating the overall material response under simple loading conditions.

Many modeling techniques have been introduced to provide either rigorous bounds or approximate predictions. Details can be found at reference [27]. In this chapter, a brief description of homogenization using representative volume element (RVE) analysis has been given. A short description of MSG homogenization technique has followed the RVE analysis.

4.1.1 Microstructure, Representative Volume Element and Unit Cell

The very first step of micromechanics is to select the right microstructure. The fundamental requirement is that the micromechanics model should be representative of the material of which the macroscopic structure can be considered to be made of. In general, there are four ways to obtain a microstructure for the purpose of micromechanics modeling.

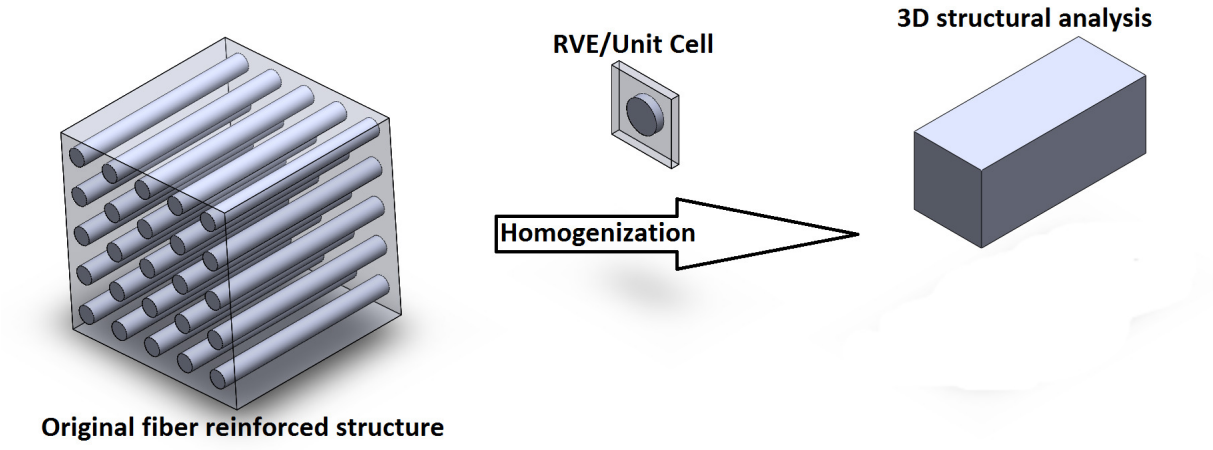

Fig. 4.1: Basic Idea of Micromechanics

First, one can use simple geometric models such as composite cylinders assembly, square or hexagonal pack microstructure for continuously fiber reinforced composites etc.

Second, one can reconstruct a microstructure based on the statistical information such as correlation functions obtained from the corresponding real microstructure.

Third, reconstruction of microstructure using image data obtained using techniques such as using X-ray microtomography.

Fourth, predicting the microstructure from simulating the manufacturing process.

The predictability of any micromechanics depends on how wisely a microscopic domain representative of the heterogeneous material, popularly known as representative volume element (RVE) is being selected. According to reference [27], an RVE is defined as any block of material the analyst wants to use for the micromechanical analysis to find the effective properties to replace it with an equivalent homogeneous material.

The term unit cell (UC) is also extensively used and sometimes used interchangeably in the literature with the RVE. A UC can be described as a fundamental building block of the material, specially if the material is periodically heterogeneous. That means, by repeating the UC for many times, the original heterogeneous material can be constructed.

Micromechanics fundamentally assumes that the heterogeneous material is at least locally periodic, where UC or RVE is defined. Another point that should be mentioned here is that, the choice of RVE or UC is not unique, even for periodic materials. Interested readers are suggested to read reference [27].

4.2 Homogenization Theory

To find effective mechanical properties of composite materials, the effective stiffness matrix or the effective compliance matrix needs to be determined. To compute the effective stiffness matrix or the effective compliance matrix, microscopic stress and strain need to be related with the macroscopic stress and strain, respectively. Often in most micromechanic models, macroscopic stresses or strains or a combination of their components are applied to the RVE usually in terms of traction boundary conditions or displacement boundary conditions, to solve a boundary value problem to find the microscopic stress and strain field within the RVE [27]. Among other modeling techniques, RVE analysis using periodic boundary condition (PBC) and MSG have been described here in brief. Between them the first one is mostly used in the literature, while the second one is a new innovation developed in Purdue University.

RVE Analysis Using PBC

Three types of boundary conditions are commonly applied to an RVE including homogeneous displacement boundary conditions, homogeneous traction boundary conditions and PBCs. It has been theoretically justified and numerically proved that PBC is the best boundary conditions to use for RVE analysis [27]. In real analysis, unit value is applied to one component of the macrocsopic strain. For example, $\bar{\epsilon}_{11} = 1$ is applied, boundary conditions for each surfaces are written out explicitly, FEA is run using these boundary conditions to carry out the static analysis to compute the stress field σ_{ij} within the RVE. Now we can compute the volume average of the stress, $\overline{\sigma}_{ij}$, which is macroscopic stress and corresponds to the first column of the effective stiffness matrix. Following the same fashion, applying unit value to the rest of five macroscopic strain components, namely, $\bar{\epsilon}_{22} = 1$,

$\bar{\epsilon}_{33} = 1$, $\bar{\gamma}_{12} = 1$, $\bar{\gamma}_{13} = 1$, $\bar{\gamma}_{23} = 1$, corresponding column of the effective stiffness matrix can be obtained. Six FEA static analyses are needed to compute the fully populated 6×6 stiffness matrix.

Mechanics of Structure Genome (MSG)

A genome serves as a blueprint for an organism's growth and development. This word can be extrapolated into nonlogical contexts to connote a *fundamental building block* of a system. Mechanics of structure genome (MSG) is a unified approach recently introduced for multi-scale constitutive modeling for all types of composites structures including beams, plates/shells and 3D structures [27]. A structure genome (SG) is defined as the smallest mathematical building block of the structure, to emphasize the fact that it contains all the constitutive information needed for a structure in the same fashion that the genome contains all the genetic information for an organism's growth and development.

For 3D structures, the SG serves a similar role as the RVE in micromechanics (Figure 4.2). However, they are significantly different. That's why the new term (SG) is used to avoid confusion. For example, for a structure made of composites featuring 1D heterogeneity, (e.g. binary composites made of two alternating layers, first image of Figure 4.2), the SG will be a straight line with two segments denoting corresponding phases. If the 1D SG is repeated in-plane for several times, the in-plane 2D binary composite with two layers can be formed. Now by repeating the 2D binary composite out-of-plane for several times, the whole 3D structure can be formed. The constitutive modeling over the 1D SG can compute the complete set of 3D properties and local fields. Such applications of the SG are not equivalent to the RVE. For a structure made of composites featuring 2D heterogeneity (e.g. continuous unidirectional fiber reinforced composites, second image of Figure 4.2), the SG will be 2D. Again, unlike 2D RVE, 2D SG can give the complete set of 3D properties and local fields for 3D structural analysis. A 2D RVE gives only in-plane properties and local fields. To get the complete set of properties for 3D structural analysis, a 3D RVE is usually required [28]. For a structure made of 3D heterogeneity (e.g. particle reinforced

composites, third image of Figure 4.2), the SG will be a 3D volume. Even though a 3D SG for 3D structures represents the most similar case to an RVE, indispensable boundary conditions in terms of displacements and traction in RVE-based models are not required for SG-based models. Clearly, SG uses the lowest dimension, thus highest efficiency, to describe the heterogeneity, while RVE dimension usually is determined by heterogeneity as well as by what type of properties required for the structural analysis. Although unnecessary waste

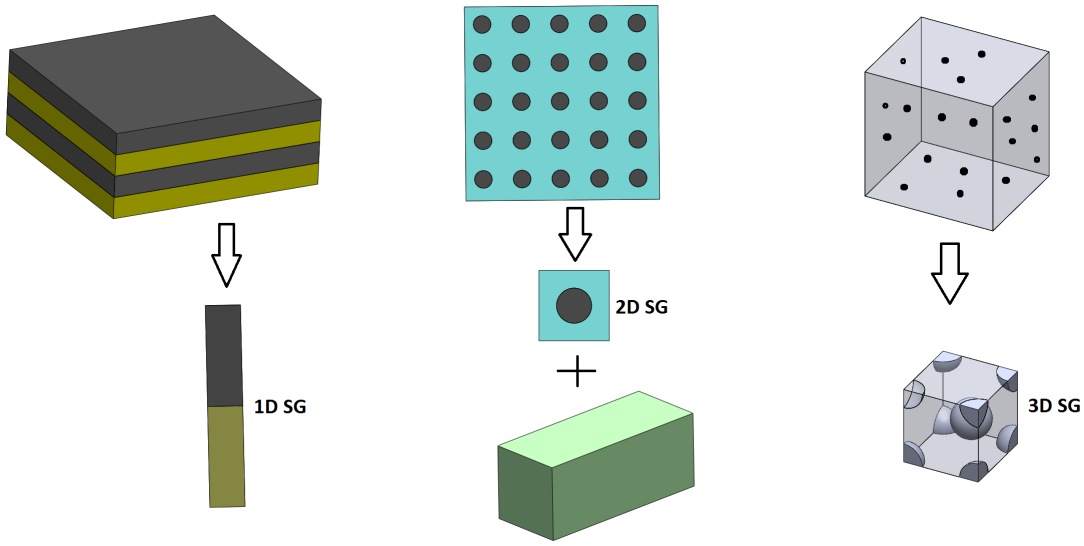

Fig. 4.2: SG for 3D Structures

of computing resources, MSG can use SGs with higher dimensions to reproduce the results by SGs with dimensionality the same as that of the heterogeneity. For example, MSG can use 2D or even 3D SGs to reproduce the results of 1D SGs for binary composites. Similarly, MSG can use 3D SGs to reproduce the results of 2D SGs for continuous fiber reinforced composites.

As far as efficiency is concerned, computing the complete stiffness matrix, RVE analysis requires solving the six static problems because the coefficient matrix of the linear system is

affected by the coupled equation constraints used to apply the periodic boundary conditions. MSG can be implemented using the finite element method so that the linear system will be factorized once and solved for six load steps. Theoretically speaking, MSG could be five to six times more efficient than RVE analysis. For detailed mathematical formulation of MSG, interested readers are refered to [27].

4.3 Effective properties of Flax Fiber and Jute Fiber

The purpose of this section is to evaluate the effective properties (independent elastic constants) of flax fiber and jute fiber. The goal can be achieved in two steps -

1. By calculating elastic properties of cell wall layers - M, P, S1, S2, S3. To do this, elastic properties of constituents need to be known. From now on, by saying constituents, we will mean cellulose, hemicellulose and lignin. Volume fraction of the constituents and their spiral angle with respect to fiber axis also need to be known.

2. By calculating elastic properties of cell wall, which consists of M, P, S1, S2 and S3 with respective volume fraction.

4.3.1 Structure of Cell Wall in Bast Fibers

Cell wall of bast fibers can be observed from two length scales, namely nanoscale, and microscale (Figures 4.3 and 4.4). At nanoscale, cell wall consists of cellulose, hemicellulose and lignin. Cellulose acts as fiber embedded in the matrix of hemicellulose + lignin. In fact, cellulose is spirally wound in a matrix of amorphous hemicellulose + lignin, as shown in Figure 4.5. At microscale, cell wall consists of five layers, namely M, P, S1, S2 and S3 layers (Figure 4.3). S1, S2 and S3 layers are called secondary layers, which together occupy as much as 92% of the cell wall structure [29]. In fact, S2 layer let alone occupies 76-80% of the total volume of cell wall [2, 29]. Just not to get confused with cell wall and cell wall layers, M, P, S1, S2 and S3 are *cell wall layers* while these five layers together make the *cell wall*.

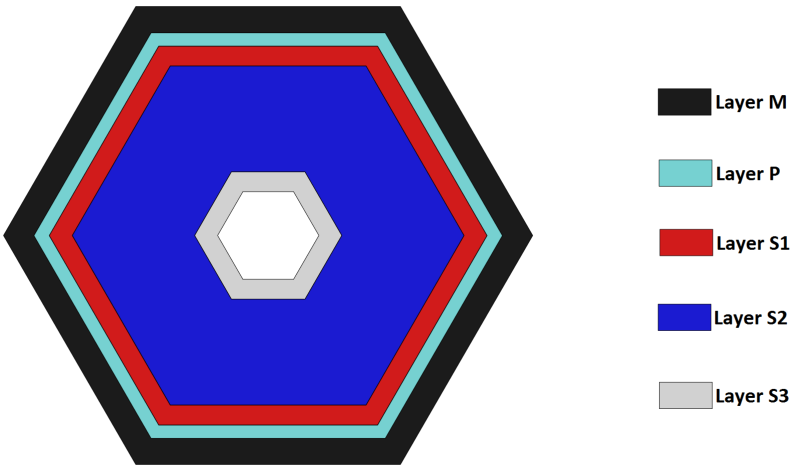

Fig. 4.3: A View of Cell Wall Layers M, P, S1, S2, S3

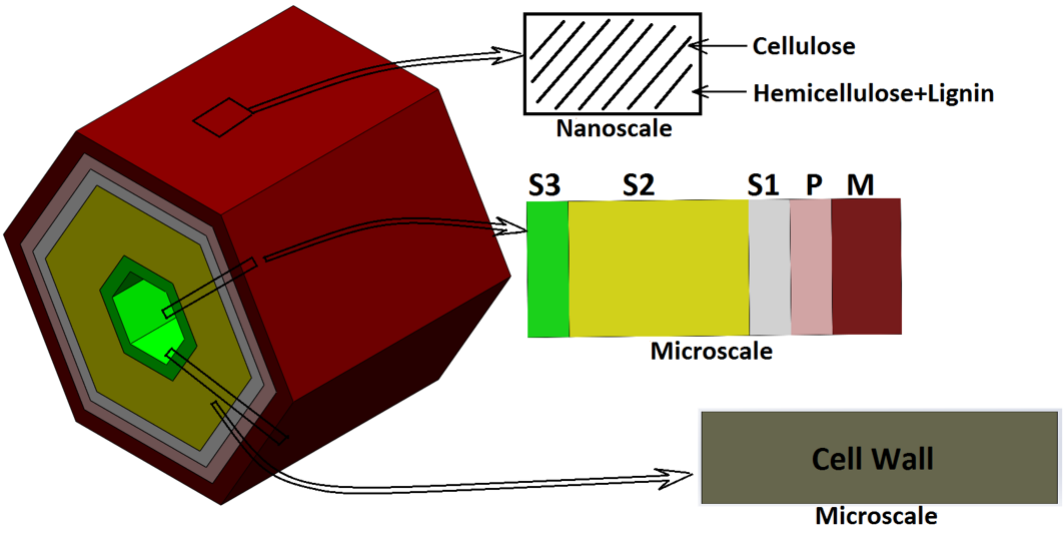

Fig. 4.4: View of Cell Wall from Different Length Scale

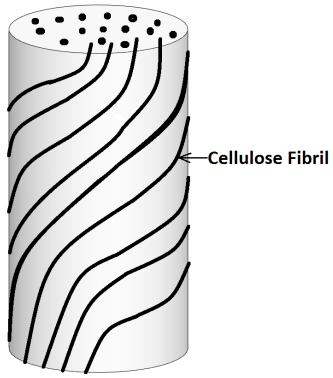

Fig. 4.5: Helical Arrangement of Cellulose (fibril) in Amorphous Hemicellulose-Lignin Matrix

4.3.2 Geometry and Properties of Constituents

To evaluate effective properties of cell wall layers, effective properties of constituents as well as volume fraction of each constituent in each layer are important. Table 4.1 provides the effective properties of constituents which has been collected from [1]. Following the same procedure followed by Qing *et. al.*, we have used square shaped RVE of cell wall layers with three concentric layers [1]. From the inner most to the outer most, the layers are cellulose, hemicellulose and lignin, respectively (Figure 4.6).

Table 4.1: Elastic Constants of Constituents (Cellulose, Hemicellulose, Lignin) [1]

Material	E_1 (MPa)	E_2 (MPa)	G_{12} (MPa)	ν_{12}	ν_{23}
Cellulose	138000	27200	4400	0.235	0.48
Hemicellulose	7000	3500	1800	0.2	0.4
Lignin	2000	2000	770	0.3	0.3

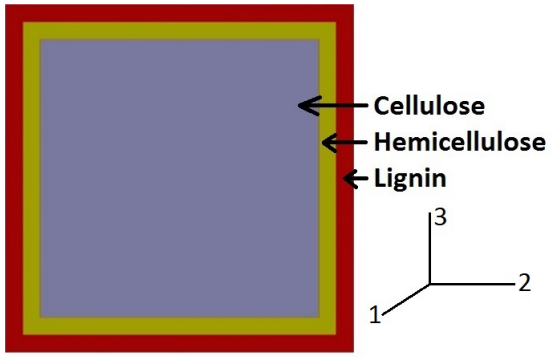

Fig. 4.6: Square RVE of Cell Wall Layer with Cellulose, Hemicellulose and Lignin

4.3.3 Finite Element Modeling

The bulk of the cell wall of bast fibers is made of S2 layer (76-80% in volume). That's why here it is assumed that cell walls of both flax and jute fiber are made of S2 layers only. This assumption makes the problem much simpler, without compromising the accuracy of the calculated effective properties of the cell walls. Cellulose content, as well as spiral angle of cellulose in S2 layer of different fibers are collected from [2] and given in table 4.2. For S2 layer of flax, volume fraction of cellulose, hemicellulose and lignin are considered to be 71%, 25% and 4% respectively, while for S2 layer of jute, cellulose, hemicellulose and lignin are considered to be 61%, 35% and 4% respectively. Geometry and meshing of the square unit cell (Figure 4.6) are done in SWIFTCOMP GUI, an FEA based free online tool developed at Purdue University. SWIFTCOMP GUI uses MSG for homogenization [30]. The calculated effective properties of S2 layers of flax and jute fiber are given in Table 4.3 and 4.4 respectively.

Once effective properties of S2 layers of flax and jute are evaluated, it is quite straight forward to calculate the effective properties of flax fiber and jute fiber. It can be done in two steps like following -

1. Drawing an RVE of flax and jute fibers. It is assumed that the cell walls of both of them consist of S2 layers only and lumens at the center of the fiber cells.

2. Rotating effective properties of S2 layers from cellulose axis $(L-T)$ to fiber axis $(X-Y)$ as shown in Figure 4.7. In the figure, θ is the angle between cellulose axis and fiber axis. θ for different fibers are given in [2] and showed in table 4.2. After axis rotation, homogenization of the RVE is carried out which yields the effective properties of flax and jute fibers.

Most of the natural fibers are hexagonal in shape. An SEM image of flax fiber is shown in Figure 4.8. Another SEM image of bundle of jute fibers is shown in Figure 4.9. In our RVE modeling, we have also used hexagonal RVE for both flax and jute fibers. RVE of flax and jute are showed in Figures 4.10 and 4.11, respectively.

Volume fraction of lumens in flax and jute fiber are considered to be 4% and 24.3% respectively [29, 31]. Value of θ for flax and jute fibers are considered to be 10^o and 8^o respectively [2]. Mathematics behind the rotation of axis is given in Appendix. Calculated elastic properties of flax and jute are given in Table 4.5 and 4.6, respectively. Finally effect of θ, angle between cellulose axis and fiber axis, on E_1 value of flax fiber is demonstrated in Figure 4.12. It is clearly evident that with increase of angle with fiber axis, E_1 decreases. It is because, with the increase of angle between cellulose axis and fiber axis, cellulose becomes more aligned with the transverse direction of the fiber. That is why, longitudinal elastic modulus, E_1 decreases. For the same reason transverse elastic modulus, E_2 increases.

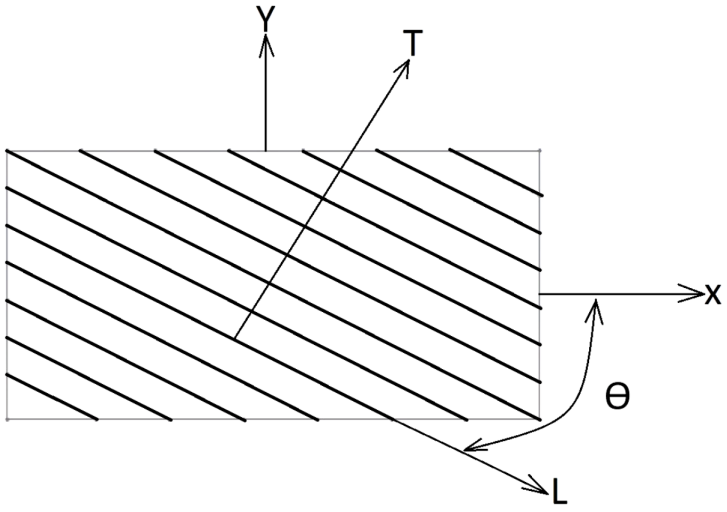

Fig. 4.7: Angle θ Between Cellulose Axis and Fiber Axis

Table 4.2: Cellulose Content and Spiral Angle of S2 Layer in Different Natural Fibers [2]

Fiber	Spiral Angle [deg]	Cellulose content [wt %]
Banana	11	65
Coir	30-49	43
Flax	6-10	64-71
Hemp	6	-
Jute	8	61-72
Pineapple	8-14	81
Sisal	10-25	66-70
Ramie	8	69-83

Table 4.3: Elastic Constants of S2 Layer of Flax Fiber

E_1 (GPa)	E_2 (GPa)	E_3 (GPa)	G_{12} (GPa)	G_{13} (GPa)	G_{23} (GPa)	ν_{12}	ν_{13}	ν_{23}
99.68	12.35	12.35	3.15	3.15	3.10	0.229	0.229	0.318

Table 4.4: Elastic Constants of S2 Layer of Jute Fiber

E_1 (GPa)	E_2 (GPa)	E_3 (GPa)	G_{12} (GPa)	G_{13} (GPa)	G_{23} (GPa)	ν_{12}	ν_{13}	ν_{23}
86.91	10.13	10.13	2.89	2.89	2.59	0.227	0.227	0.316

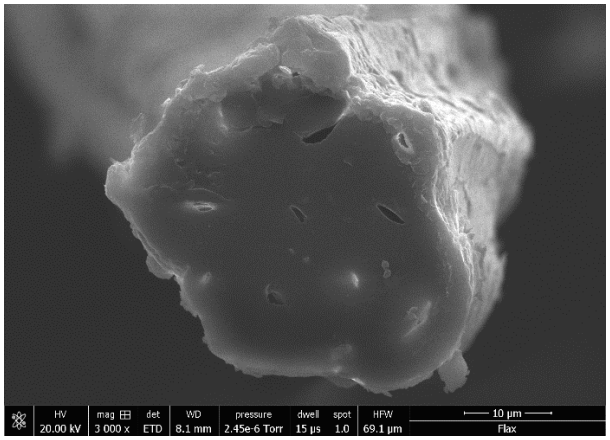

Fig. 4.8: SEM Image of Flax Fiber

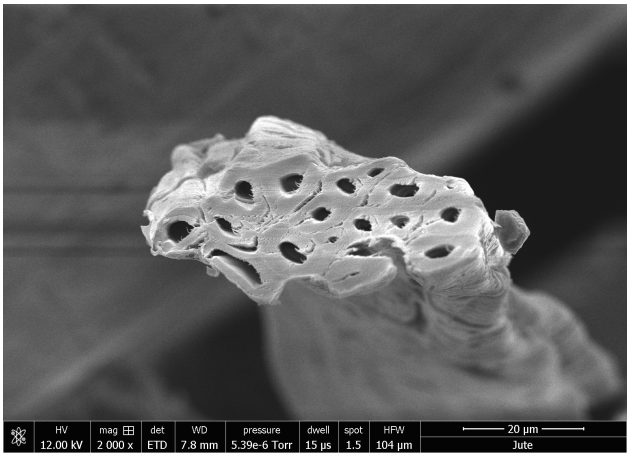

Fig. 4.9: SEM Image of Jute Fiber Bundle

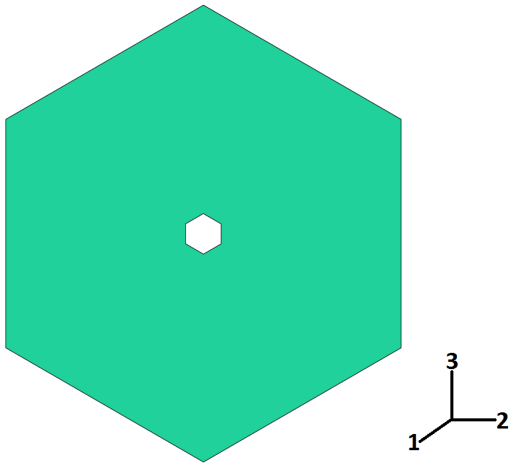

Fig. 4.10: RVE of Flax Fiber

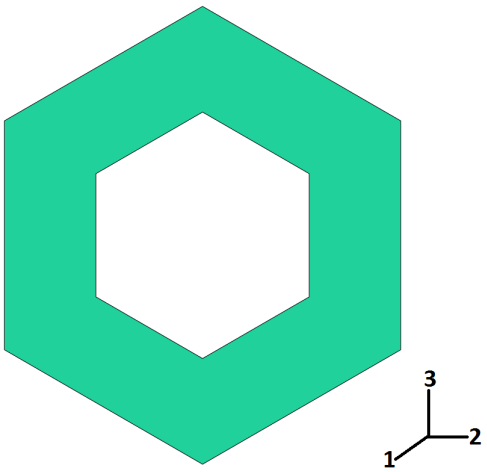

Fig. 4.11: RVE of Jute Fiber

Table 4.5: Elastic Constants of Flax Fiber

E_1 (GPa)	E_2 (GPa)	E_3 (GPa)	G_{12} (GPa)	G_{13} (GPa)	G_{23} (GPa)	ν_{12}	ν_{13}	ν_{23}
52.04	10.61	11.49	3.17	2.92	2.75	0.473	0.161	0.279

Table 4.6: Elastic Constants of Jute Fiber

E_1 (GPa)	E_2 (GPa)	E_3 (GPa)	G_{12} (GPa)	G_{13} (GPa)	G_{23} (GPa)	ν_{12}	ν_{13}	ν_{23}
43.56	5.52	5.64	1.79	1.71	0.85	0.401	0.180	0.192

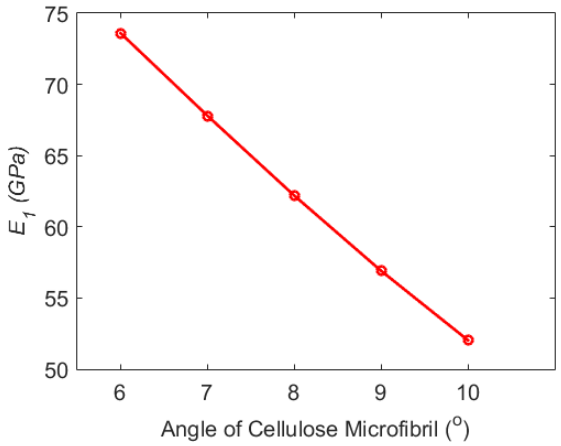

Fig. 4.12: Effect of Angle Between Cellulose Axis and Fiber Axis on E_1 Value of Flax Fiber

4.3.4 Comparison Between Numerical and Analytical Results of S2 Layer

In this section, numerically computed effective properties of S2 layers of flax and jute are compared with the analytical results. In [1], authors have used a double pass homogenization technique. But multi-pass homogenization technique violates equilibrium and compatibility requirements [32]. That's why we have developed a new single pass homogenization technique. Following, single pass homogenization technique and associated equations are described elaborately. Double pass homogenization technique is also given in brief. Numerical results calculated using FEM based MSG are compared with analytical results evaluated using single pass homogenization. In the graphs, the FEM based MSG is denoted as *MSG*. Finally, a comparison between calculated effective properties by single pass homogenization and double pass homogenization has been provided.

Single Pass Homogenization

In single pass homogenization, all three constituents, namely cellulose, hemicellulose and lignin are concentric being from inner most to the outer most layer respectively (Figure 4.13). E_1, ν_{12} and ν_{13} are calculated using rule of hybrid mixture (RoHM) equations, where as E_2, E_3, G_{12}, G_{13} and G_{23} are calculated using modified Halpin-Tsai equations.

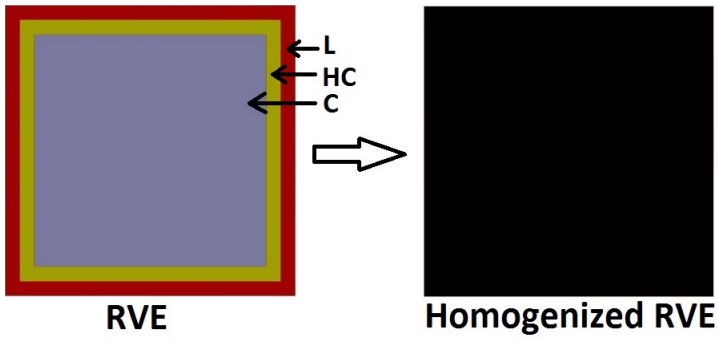

Fig. 4.13: A One Step Homogenization Procedure for the RVE of Cell Wall

RoHM equations are developed following reference [22] and are given below.

$$E_1 = E_{1(C)}V_C + E_{1(HC)}V_{HC} + E_{1(L)}V_L \tag{4.1}$$

$$\nu_{12} = \nu_{12(C)}V_C + \nu_{12(HC)}V_{HC} + \nu_{12(L)}V_L \tag{4.2}$$

$$\nu_{13} = \nu_{13(C)}V_C + \nu_{13(HC)}V_{HC} + \nu_{13(L)}V_L \tag{4.3}$$

Here, $'C'$, $'HC'$ and $'L'$ stand for cellulose, hemicellulose and lignin, respectively. $E_{1(C)}$, $E_{1(HC)}$, and $E_{1(L)}$ refer to the longitudinal modulus values for cellulose, hemicellulose and lignin respectively, and V_C, V_{HC}, and V_L refer to the volume fraction of cellulose, hemicellulose and lignin respectively.

Transverse modulus E_2 and E_3, however can't be predicted accurately using equations of the form 4.1. To calculate them, semi-empirical equation like Halpin-Tsai equation is used. The Halpin-Tsai equation for single fiber composite is [22]

$$\frac{E_2}{E_m} = \frac{1 + \eta\Psi V_f}{1 - \eta V_f} \tag{4.4}$$

where

$$\eta = \frac{\gamma + 1}{\gamma + \Psi} \tag{4.5}$$

and

$$\gamma = \frac{E_f}{E_m} \tag{4.6}$$

In the equations above, $'f'$ stands for fiber and $'m'$ stands for matrix. Ψ is a curve-fitting parameter, which is dependent on the fiber packing arrangement. For the RVE of

cell wall, a modified Halpin-Tsai equation is proposed here, which incorporates the volume fractions of all the reinforcements as follows:

$$\frac{E}{E_L} = \frac{1 + \Psi(\eta_C V_C + \eta_{HC} V_{HC})}{1 - (\eta_C V_C + \eta_{HC} V_{HC})} \tag{4.7}$$

where

$$\eta_C = \frac{(E_C/E_L) - 1}{(E_C/E_L) + \Psi} \tag{4.8}$$

$$\eta_{HC} = \frac{(E_{HC}/E_L) - 1}{(E_{HC}/E_L) + \Psi} \tag{4.9}$$

Here E refers to transverse moduli E_2 and E_3. For each case, the corresponding fiber (cellulose and hemicellulose) transverse moduli have to be considered to calculate the parameter η. J. C. Halpin and co-authors suggested that reliable estimates for Ψ factor could be obtained by comparison of the Halpin-Tsai equations with the numerical micromechanics solutions employing the formal elasticity theory [33]. The optimum value of Ψ is found to be 2.2 for calculating E_2 and E_3, which yielded the best match in between the analytical results and the numerical solution.

To calculate shear moduli G_{12}, G_{13} and G_{23}, the same procedure of calculating transverse modulus can be adopted. The modified Halpin-Tsai relation for predicting the shear moduli is given below -

$$\frac{G}{G_L} = \frac{1 + \Psi(\eta_C V_C + \eta_{HC} V_{HC})}{1 - (\eta_C V_C + \eta_{HC} V_{HC})} \tag{4.10}$$

where

$$\eta_C = \frac{(G_C/G_L) - 1}{(G_C/E_L) + \Psi} \tag{4.11}$$

$$\eta_{HC} = \frac{(G_{HC}/G_L) - 1}{(G_{HC}/G_L) + \Psi} \tag{4.12}$$

In the above equation, G refers to shear modulus (G_{12}, G_{13}, G_{23}) of the RVE. For each case, the corresponding fiber (cellulose and hemicellulose) shear moduli have to be considered in calculating the parameter η. The optimal value of Ψ is used as 1.2 for G_{12} and G_{13} and 0.1 for G_{23}.

Double Pass Homogenization

Rule of mixture equation is used to calculate the value of E_1, ν_{12} and ν_{13}, whereas Tsai-Hahn equation is used to calculate the value of E_2, E_3, G_{12}, G_{13} and G_{23}. Dayakar and co-authors used Tsai-Hahn equation to calculate transverse Young's modulus and reported that it gave better approximation when compared to 3D FEA [34]. Unlike single pass homogenization, in case of Tsai-Hahn equation, a double pass homogenization technique has been used. In the first pass, the hemicellulose is considered to be the fiber embedded in lignin. The elastic constants calculated in this way have been used as the matrix property in the second pass where cellulose fiber is embedded in a matrix of homoegenized hemicellulose+lignin (Figure 4.14). The opposite is also possible. That means in the first pass, cellulose and hemicellulose can be considered as fiber and matrix respectively. In the second pass, homogenized cellulose+hemicellulose can be considered as a fiber embedded in the lignin matrix.

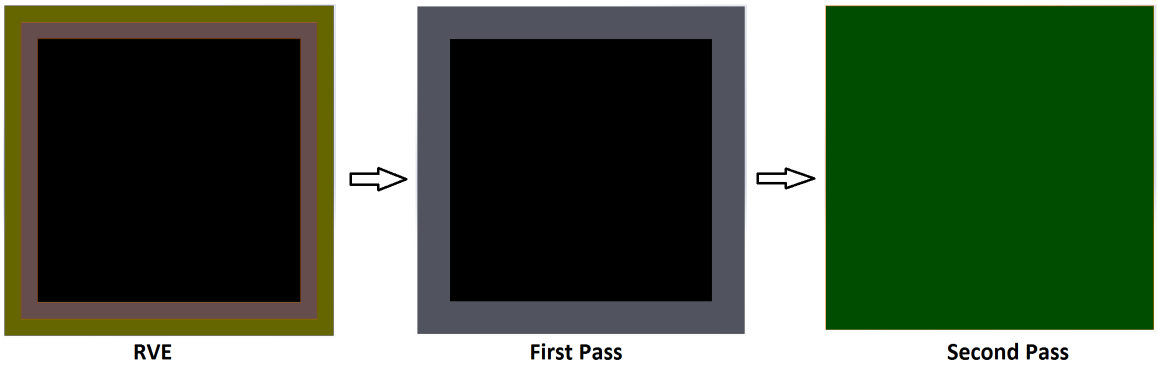

Fig. 4.14: A Two Step Homogenization Procedure for the RVE of Cell Wall

Rule of mixture (RoM) equations are given below.

$$E_1 = E_{1(C)}V_C + E_{1(HC)}V_{HC} + E_{1(L)}V_L \tag{4.13}$$

$$\nu_{12} = \nu_{12(C)}V_C + \nu_{12(HC)}V_{HC} + \nu_{12(L)}V_L \tag{4.14}$$

Tsai-Hahn equations are given below.

$$\frac{1}{E} = \frac{1}{V_f + \eta V_m}(\frac{V_f}{E_f} + \eta\frac{V_m}{E_m}) \quad where \quad \eta = 0.47 \tag{4.15}$$

$$\frac{1}{G} = \frac{1}{V_f + \eta V_m}(\frac{V_f}{G_f} + \eta\frac{V_m}{G_m}) \quad where \quad \eta = 0.47(1 + \frac{G_m}{G_f}) \tag{4.16}$$

Here $'f'$ stands for fiber and $'m'$ stands for matrix. Similarly, E stands for E_2, E_3 and G stands for G_{12}, G_{13}, G_{23}. In the first pass, hemicellulose is the fiber and lignin is the matrix. In the second pass cellulose is the fiber and homogenized hemicellulose+lignin is the matrix. v_{23} can be calculated using the following equation due to the transverse isotropic behavior of the RVE.

$$G_{23} = \frac{E_2}{2(1+\nu_{23})} \tag{4.17}$$

Where, the values of E_2 and G_{23} have already been calculated using Tsai-Hahn equations.

Comparison for S2 Layer of Flax

Numerical results of elastic constant of S2 layer of flax are compared with analytical results and are given in Table 4.7. The values given in Table 4.7 are calculated for 71%, 25% and 4% volume fraction of cellulose, hemicellulose and lignin respectively. Effect of cellulose content on the effective properties of S2 layer has also been demonstrated graphically in Figure 4.15-4.19 for E_1, E_2 & E_3, G_{12} & G_{13}, G_{23}, ν_{12} & ν_{13}. Graph showing effect of cellulose content on ν_{23} is not provided, due to the reason that it can readily be calculated from G_{23} and E_2 due to the transversely isotropy of S2 layer.

Table 4.7: Comparison of Elastic Constants in S2 Layer of Flax

	E_1 (GPa)	E_2 (GPa)	G_{12} (GPa)	G_{23} (GPa)	ν_{12}
Numerical(MSG)	99.68	12.35	3.15	3.10	0.229
Analytical	99.81	12.05	3.08	3.13	0.229

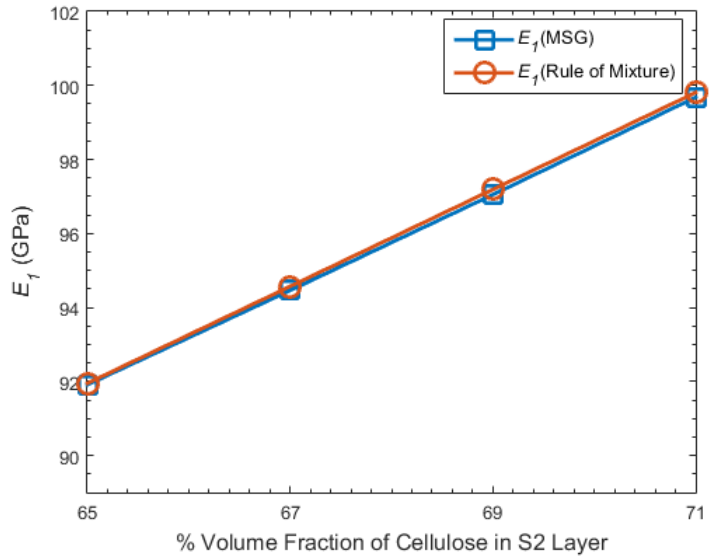

Fig. 4.15: Effect of Cellulose Content on E_1 of S2 Layer of Flax

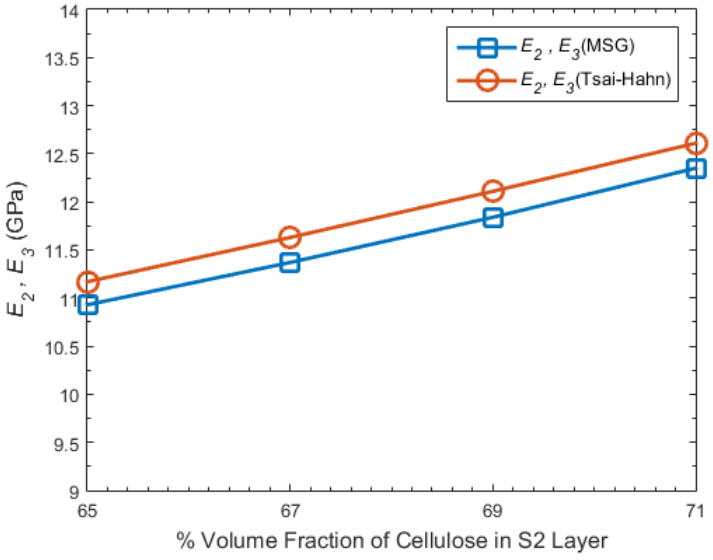

Fig. 4.16: Effect of Cellulose Content on E_2 and E_3 of S2 Layer of Flax

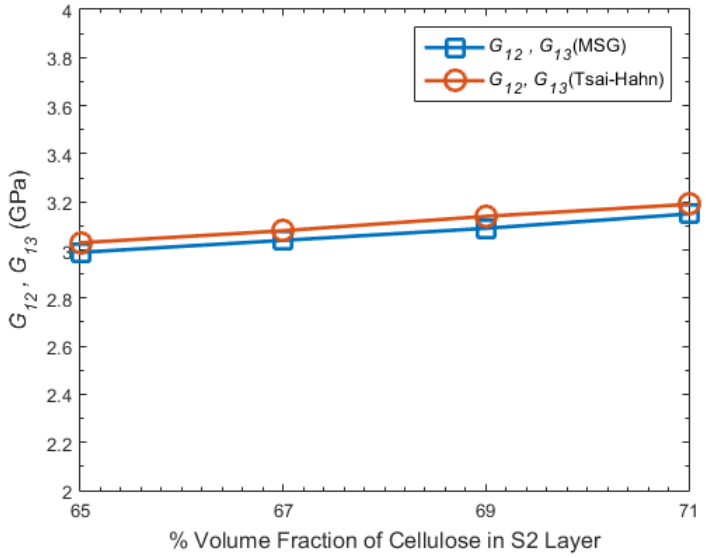

Fig. 4.17: Effect of Cellulose Content on G_{12} and G_{13} of S2 Layer of Flax

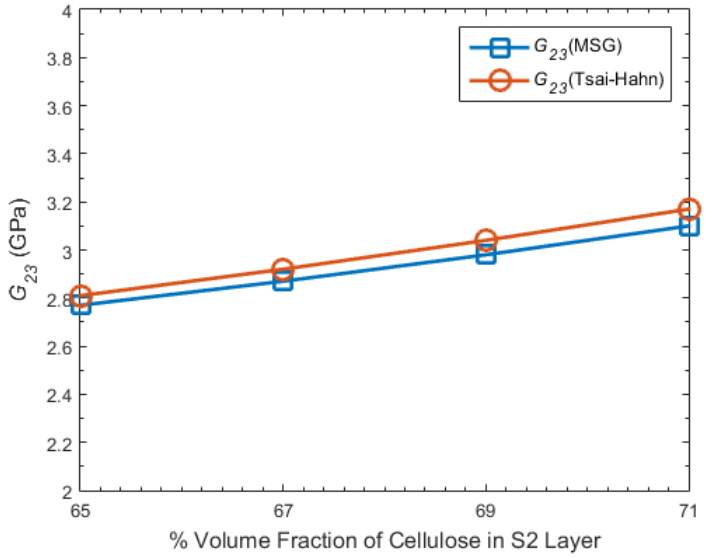

Fig. 4.18: Effect of Cellulose Content on G_{23} of S2 Layer of Flax

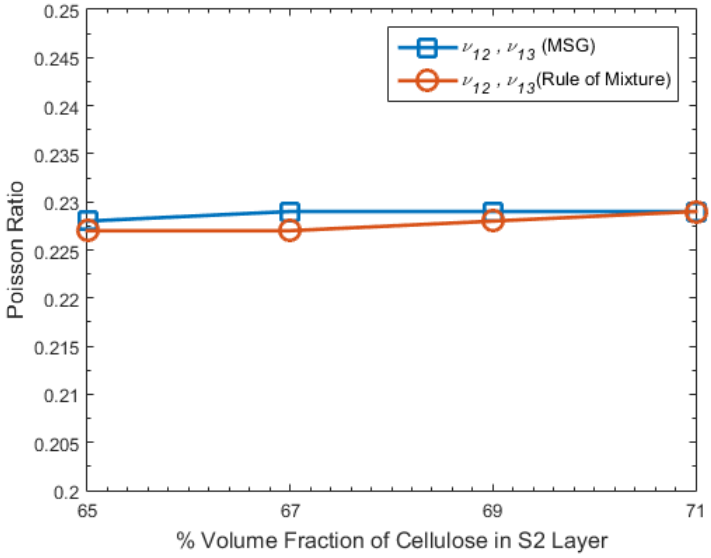

Fig. 4.19: Effect of Cellulose Content on ν_{12} and ν_{13} of S2 Layer of Flax

Observation

• All the effective mechanical properties increase with the increase of cellulose content. As cellulose is the stiffest among all three constituents, such an increase in effective properties is expectable.

Comparison for S2 Layer of Jute

Numerical results of elastic constants of S2 layer of jute are compared with analytical results and are given in Table 4.8. The values given in Table 4.8 are calculated for 61%, 35% and 4% volume fraction of cellulose, hemicellulose and lignin, respectively. Effect of cellulose content on the effective properties of S2 layer has also been demonstrated graphically in Figures 4.20-4.24 for E_1, E_2 & E_3, G_{12} & G_{13}, G_{23}, ν_{12} & ν_{13}.

Table 4.8: Comparison of Elastic Constants in S2 Layer of Jute

	E_1 (GPa)	E_2 (GPa)	G_{12} (GPa)	G_{23} (GPa)	ν_{12}
Numerical(MSG)	86.91	10.13	2.89	2.59	0.227
Analytical	86.71	9.92	2.83	2.58	0.225

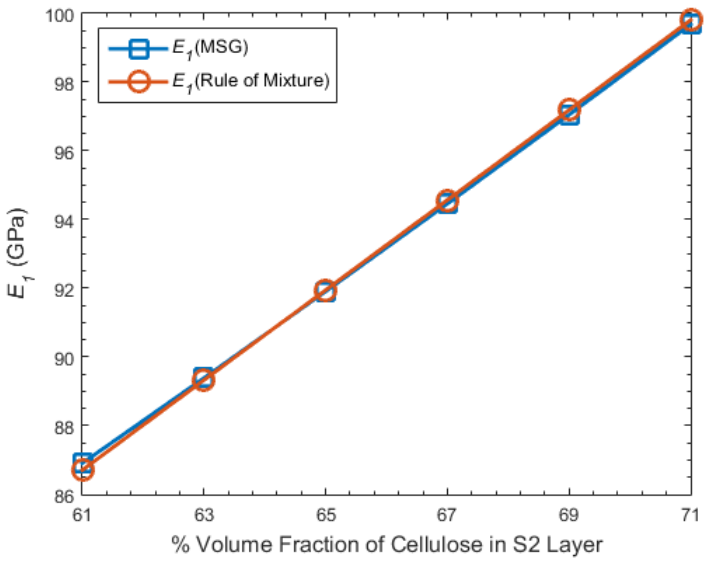

Fig. 4.20: Effect of Cellulose Content on E_1 of S2 Layer of Jute

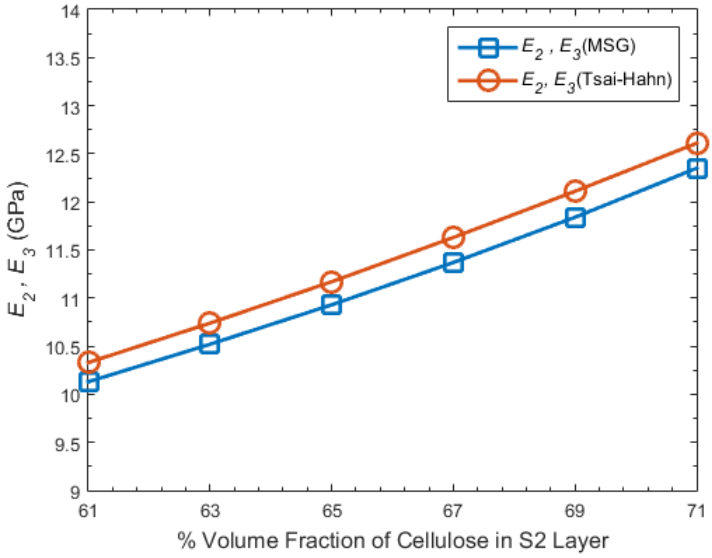

Fig. 4.21: Effect of Cellulose Content on E_2 and E_3 of S2 Layer of Jute

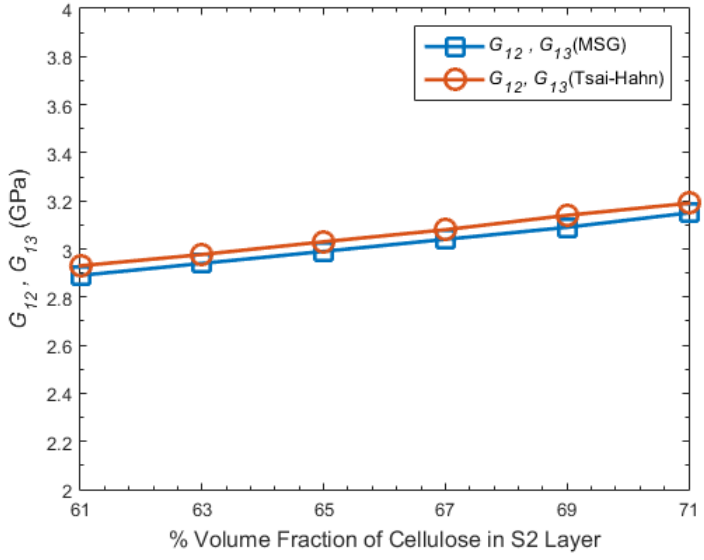

Fig. 4.22: Effect of Cellulose Content on G_{12} and G_{13} of S2 Layer of Jute

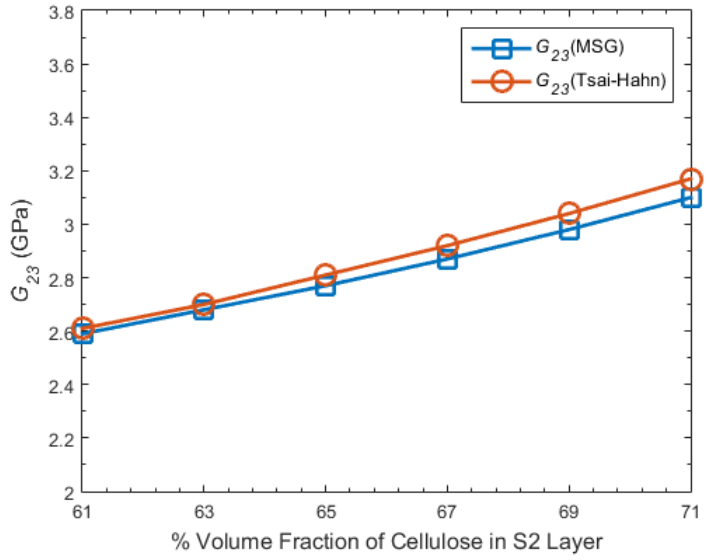

Fig. 4.23: Effect of Cellulose Content on G_{23} of S2 Layer of Jute

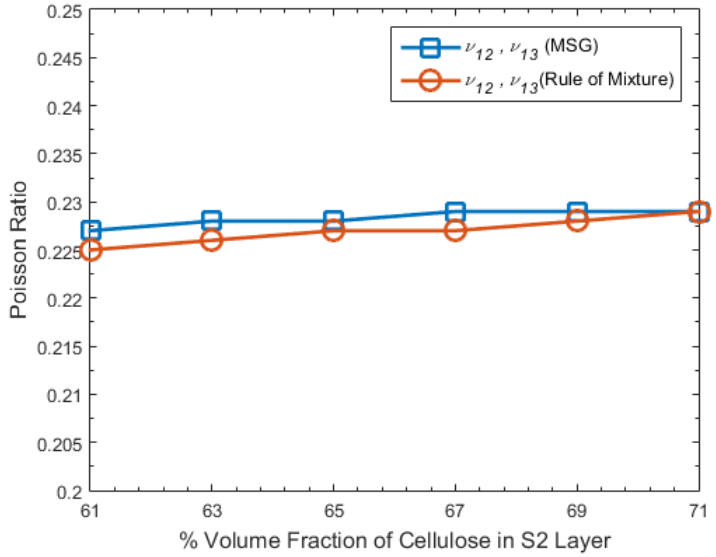

Fig. 4.24: Effect of Cellulose Content on ν_{12} and ν_{13} of S2 Layer of Jute

Observation

- All the effective mechanical properties increase with the increase of cellulose content. As cellulose is the stiffest among all three constituents, such an increase in effective properties is expectable.

Comparison Between Single Pass Homogenization and Double Pass Homogenization

To compare the single pass homogenization and double pass homogenization, E_2 & E_3 as well as G_{12} & G_{13} of flax for 71% cellulose, 25% hemicellulose and 4% lignin calculated by both of the methods are given in Table 4.9 and also showed graphically in Figures 4.25 and 4.26.

Table 4.9: E_2 & E_3 (GPa) and G_{12} & G_{13} (GPa) Calculated Using Single Pass and Double Pass Homogenization Technique

Parameter	E_2 & E_3 (GPa)	G_{12} & G_{13} (GPa)
Single pass	12.05	3.08
Double pass	12.075	3.21
% Diff (absolute)	0.21	4.05

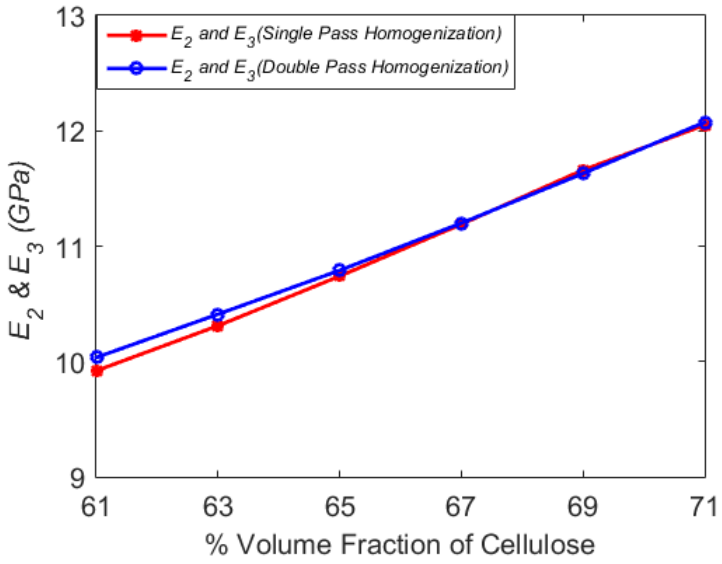

Fig. 4.25: Comparison Between Single Pass Homogenization and Double Pass Homogenization for Transverse Young Modulus

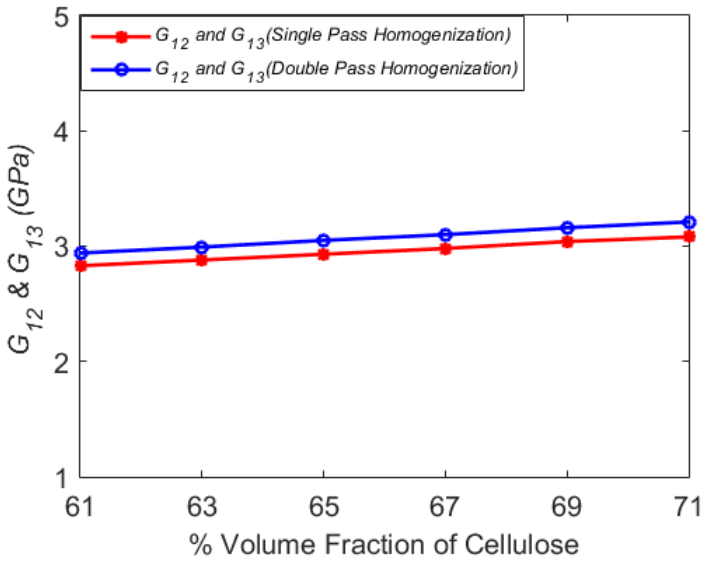

Fig. 4.26: Comparison Between Single Pass Homogenization and Double Pass Homogenization for Longitudinal Shear Modulus

Observation

• Transverse Young's moduli and longitudinal shear moduli calculated by single pass homogenization and double pass homogenization are pretty close. The differences of value calculated by two different techniques are 0.21% and 4.05% for transverse Young moduli and longitudinal shear moduli, respectively.

4.4 Effective Properties of Flax/Jute/Epoxy Hybrid Composite

In this chapter, flax and jute are embedded in the same epoxy matrix. Then by applying MSG, homogenized elastic properties of the flax/jute hybrid composite have been calculated numerically. The overall fiber volume fraction is kept constant at 30%, while relative volume fraction of flax is increased gradually (and hence relative volume fraction of jute is decreased gradually). The effect of using jute as skin material on elastic properties of the hybrid composite is also studied. The combination of flax and jute is showed in Table 4.10. Here 'F', 'J' and 'f' stands for flax, jute and fiber, respectively.

Table 4.10: Combination of Flax and Jute

Specimen	V_F	V_J	V_f
H1	0.27	0.03	0.3
H2	0.21	0.09	0.3
H3	0.15	0.15	0.3
H4	0.09	0.21	0.3
H5	0.03	0.27	0.3

4.4.1 Analytical Solution

Longitudinal modulus, E_1, and Poisson ratio ν_{12} and ν_{13} of the hybrid composite are calculated using rule of hybrid mixtures (RoHM). The equations are given below -

$$E_1 = E_{1(F)}V_F + E_{1(J)}V_J + E_{1(m)}V_m \tag{4.18}$$

$$\nu_{12} = \nu_{12(F)}V_F + \nu_{12(J)}V_J + \nu_{12(m)}V_m \tag{4.19}$$

$$\nu_{13} = \nu_{13(F)}V_F + \nu_{13(J)}V_J + \nu_{13(m)}V_m \tag{4.20}$$

Here, $'F'$, $'J'$ and $'m'$ stand for flax, jute and matrix (epoxy) respectively. $E_{1(F)}$, $E_{1(J)}$, and $E_{1(m)}$ refer to the longitudinal modulus values for flax, jute and epoxy, respectively, and V_F, V_J, and V_m refer to the volume fraction of flax, jute and epoxy, respectively.

Transverse modulus E_2 and E_3, however can't be predicted accurately using equations of the form 4.18. To calculate them, semi-empirical equation like Halpin-Tsai equation is used. The Halpin-Tsai equation for single fiber composite is [22]

$$\frac{E_2}{E_m} = \frac{1 + \eta\Psi V_f}{1 - \eta V_f} \tag{4.21}$$

where

$$\eta = \frac{\gamma + 1}{\gamma + \Psi} \tag{4.22}$$

and

$$\gamma = \frac{E_f}{E_m} \tag{4.23}$$

In the equations above, $'f'$ stands for fiber and $'m'$ stands for matrix. Ψ is a curve-fitting parameter, which is dependent on the fiber packing arrangement. For the hybrid composites, authors in [22] proposed a modification to the Halpin-Tsai equation, which incorporates the volume fractions of all the reinforcements as follows:

$$\frac{E}{E_m} = \frac{1 + \Psi(\eta_F V_F + \eta_J V_J)}{1 - (\eta_F V_F + \eta_J V_J)} \tag{4.24}$$

where

$$\eta_F = \frac{(E_F/E_m) - 1}{(E_F/E_m) + \Psi} \tag{4.25}$$

$$\eta_J = \frac{(E_J/E_m) - 1}{(E_J/E_m) + \Psi} \tag{4.26}$$

Here the subscript $'F'$, $'J'$ and $'m'$ refer to flax, jute and epoxy matrix respectively. E refers to transverse moduli E_2 and E_3. For each case, the corresponding fiber transverse moduli have to be considered to calculate the parameter η. The optimum value of Ψ is found to be 1.165 for calculating E_2 and E_3 including the single fiber composites.

To calculate shear moduli G_{12}, G_{13} and G_{23}, the same procedure of calculating transverse modulus can be adopted. The modified Halpin-Tsai relation for predicting the shear moduli is given below -

$$\frac{G}{G_m} = \frac{1 + \Psi(\eta_F V_F + \eta_J V_J)}{1 - (\eta_F V_F + \eta_J V_J)} \tag{4.27}$$

where

$$\eta_F = \frac{(G_F/G_m) - 1}{(G_F/E_m) + \Psi} \tag{4.28}$$

$$\eta_J = \frac{(G_J/G_m) - 1}{(G_J/G_m) + \Psi} \tag{4.29}$$

In the above equation, G refers to composite shear modulus (G_{12}, G_{13}, G_{23}). For each case, the corresponding fiber shear moduli have to be considered in calculating the parameter η. The optimal value of Ψ is used as 1.01 for G_{12} and G_{13} and 0.9 for G_{23} [22].

4.4.2 Numerical Solution

Figure 4.27 and 4.28 show the RVEs of flax/jute/epoxy hybrid composite. In Figure 4.27, flax is used as the boundary fiber (skin) while jute is used as the core fiber, and in Figure 4.28, jute is used as the boundary fiber while flax is used as core. The volume fraction of flax is gradually increased from 0 to 0.3, while the volume fraction of jute is gradually decreased from 0.3 to 0. The total fiber volume fraction is always kept at 0.3. MSG is applied in each case to calculate effective properties of the hybrid composites.

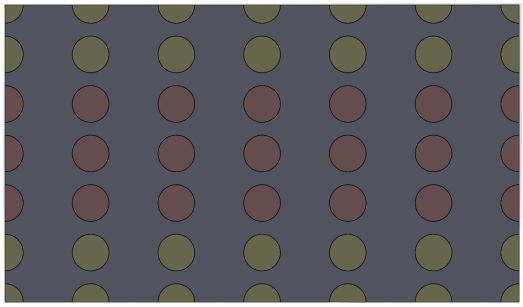

Fig. 4.27: RVE of Flax/Jute/Epoxy Hybrid Composite Where Flax is Skin, Jute is Core

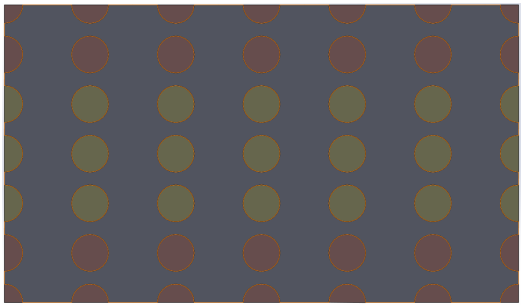

Fig. 4.28: RVE of Flax/Jute/Epoxy Hybrid Composite Where Jut is Skin, Flax is Core

4.4.3 Comparison Between Numerical and Analytical Results

Figure 4.29 shows the comparison of E_1 values calculated using MSG and RoHM. Both of the curves almost coincides establishing the accuracy of MSG. It is evident that $E1$ varies linearly with the variation of volume fraction of flax from 0 to 0.3 as we move from left to right. E_1 values of different combinations are also tabulated in Table 4.11.

Figures 4.30 and 4.31 show the variation of transverse modulus E_2 and E_3 with increasing volume fraction of flax. In both cases, MSG and modified Halpin-Tsai equation give very close results. Both E_2 and E_3 increase with the increase of flax fiber. Table 4.12 shows the difference of E_2 values calculated numerically and analytically. Similarly Table 4.13 shows the difference of E_3 values calculated numerically and analytically.

Figures 4.32, 4.33, 4.34 show the variation of G_{12}, G_{13} and G_{23} with volume fraction of

flax fiber. In all cases, MSG results conform to the modified Halpin-Tsai equations. In all cases, the values of G_{12}, G_{13} and G_{23} increase with the increase of volume fraction of flax. The increment follows a linear pattern in all cases. The values of shear modulus calculated using MSG and modified Halpin-Tsai equations are also given in Table 4.14,4.15 and 4.16.

Variation of ν_{12} with the increase of flax fiber is demonstrated in Figure 4.35 and in Table 4.17. From the figure it is evident that with the increase of volume fraction of flax fiber, value of ν_{12} increases. The variation is linear.

Change of ν_{13} with the increase of flax fiber is showed in figure 4.36 and also in table 4.18. With the increase of volume fraction of flax, value of ν_{13} decreases and the variation is linear. It is also evident that the MSG results agree with the RoHM results.

Figure 4.37 shows the variation of ν_{23} with the increase of flax fiber. With the increase of volume fraction of flax, value of ν_{23} increases. The increment follows a linear pattern. Numerical values are also given in Table 4.19.

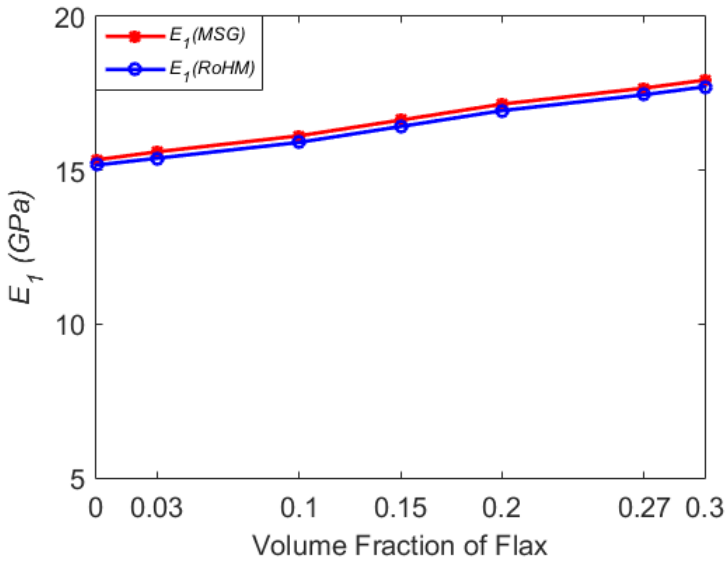

Fig. 4.29: Variation of E_1 with Volume Fraction of Flax

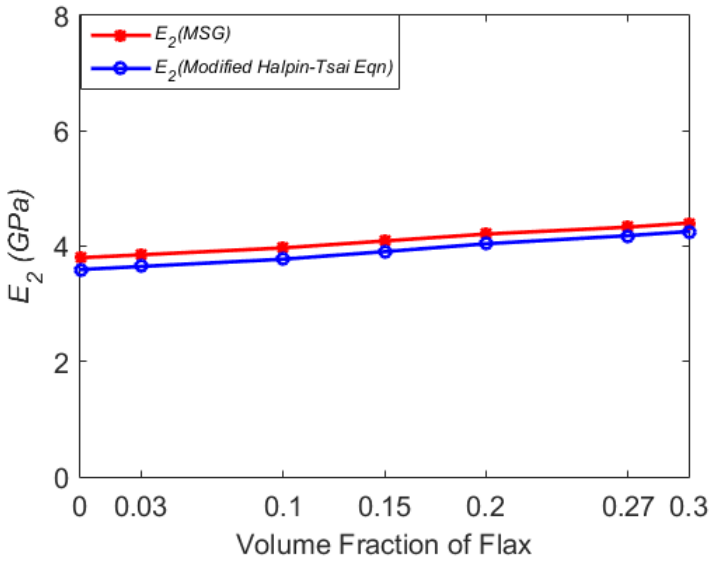

Fig. 4.30: Variation of E_2 with Volume Fraction of Flax

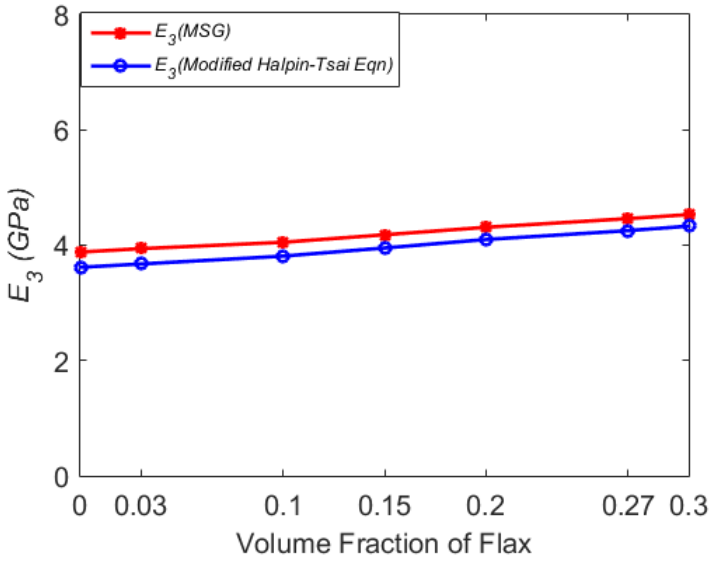

Fig. 4.31: Variation of E_3 with Volume Fraction of Flax

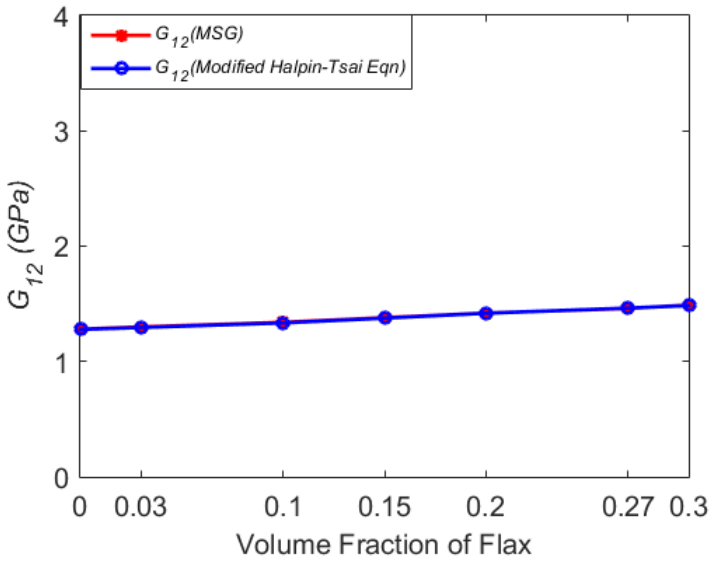

Fig. 4.32: Variation of G_{12} with Volume Fraction of Flax

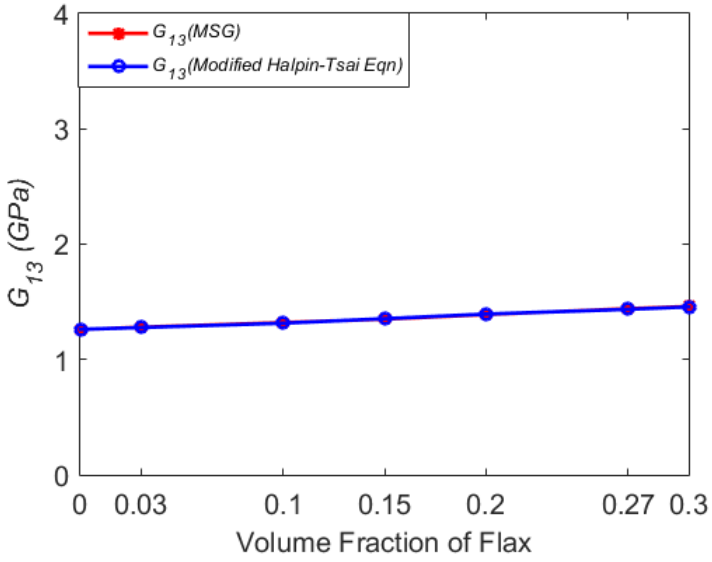

Fig. 4.33: Variation of G_{13} with Volume Fraction of Flax

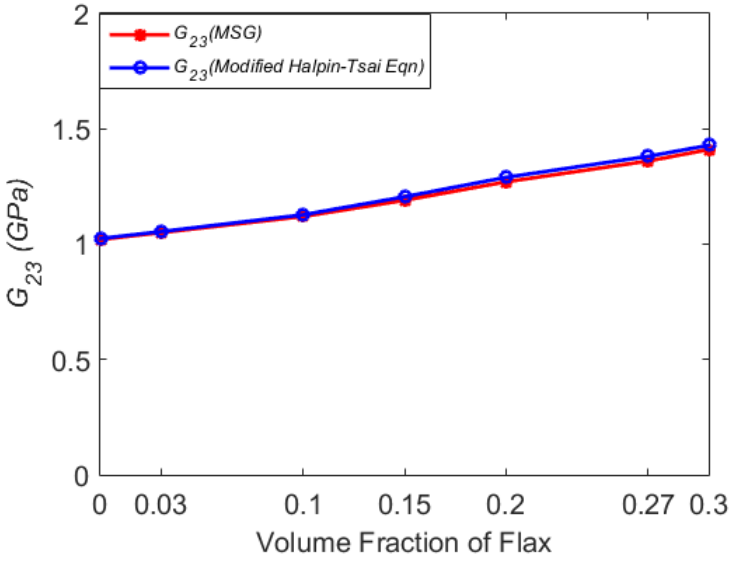

Fig. 4.34: Variation of G_{23} with Volume Fraction of Flax

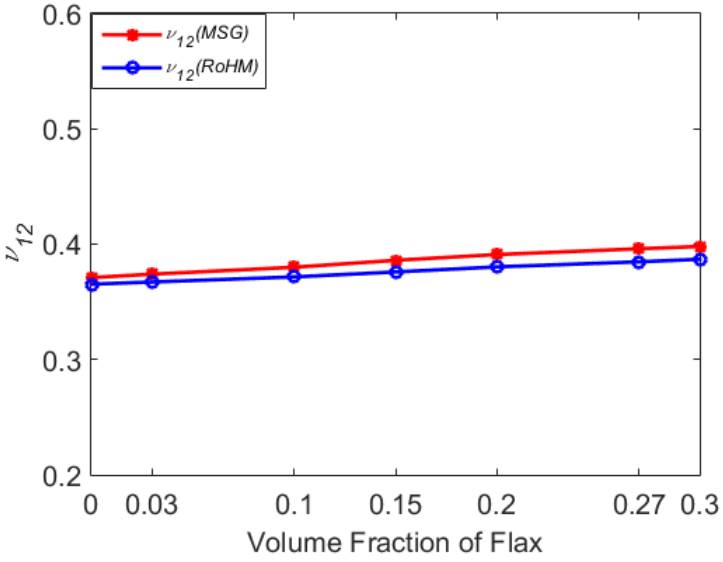

Fig. 4.35: Variation of ν_{12} with Volume Fraction of Flax

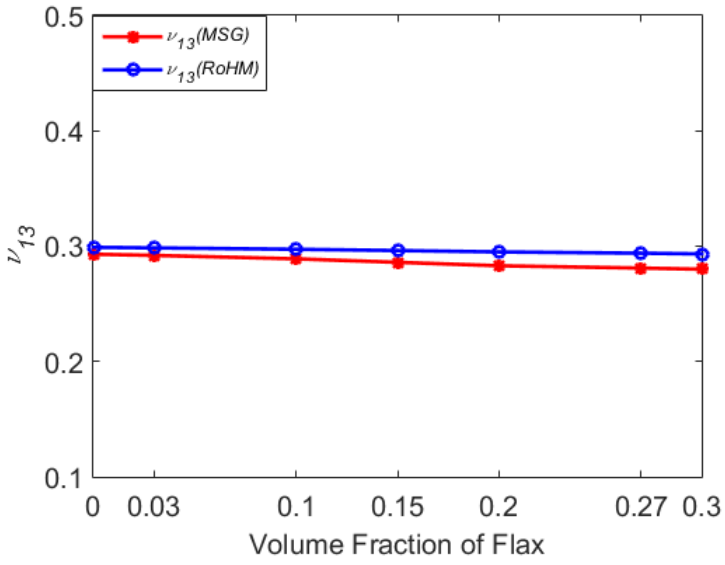

Fig. 4.36: Variation of ν_{13} with Volume Fraction of Flax

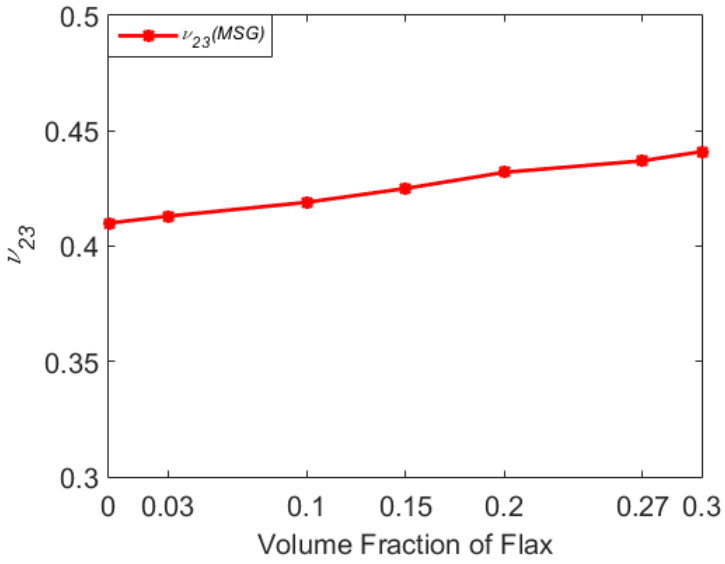

Fig. 4.37: Variation of ν_{23} with Volume Fraction of Flax

Table 4.11: E_1 (GPa) for Different Combination of Flax and Jute Given in Table 4.10

Type of composite	Flax/epoxy	H1	H2	H3	H4	H5	Jute/epoxy
MSG	17.93	17.67	17.15	16.63	16.12	15.60	15.34
RoHM	17.71	17.45	16.94	16.42	15.91	15.39	15.17
% Diff (absolute)	1.23	1.25	1.22	1.26	1.30	1.35	1.11

Table 4.12: E_2 (GPa) for Different Combination of Flax and Jute Given in Table 4.10

Type of composite	Flax/epoxy	H1	H2	H3	H4	H5	Jute/epoxy
MSG	4.36	4.30	4.18	4.05	3.94	3.81	3.76
Modified Halpin-Tsai	4.25	4.18	4.08	3.91	3.77	3.65	3.60
% Diff (absolute)	2.52	2.79	2.39	3.46	4.31	4.20	4.26

Table 4.13: E_3 (GPa) for Different Combination of Flax and Jute Given in Table 4.10

Type of composite	Flax/epoxy	H1	H2	H3	H4	H5	Jute/epoxy
MSG	4.24	4.10	3.98	3.86	3.75	3.65	3.60
Modified Halpin-Tsai	4.33	4.25	4.09	3.95	3.81	3.67	3.62
% Diff (absolute)	2.07	3.53	2.67	2.28	1.54	0.54	0.55

Table 4.14: G_{12} (GPa) for Different Combination of Flax and Jute Given in Table 4.10

Type of composite	Flax/epoxy	H1	H2	H3	H4	H5	Jute/epoxy
MSG	1.48	1.46	1.41	1.37	1.33	1.29	1.27
Modified Halpin-Tsai	1.49	1.47	1.42	1.38	1.33	1.30	1.28
% Diff (absolute)	0.67	0.68	0.70	0.72	0.0	0.77	0.78

Table 4.15: G_{13} (GPa) for Different Combination of Flax and Jute Given in Table 4.10

Type of composite	Flax/epoxy	H1	H2	H3	H4	H5	Jute/epoxy
MSG	1.41	1.38	1.34	1.31	1.27	1.24	1.22
Modified Halpin-Tsai	1.46	1.44	1.39	1.35	1.32	1.27	1.26
% Diff (absolute)	3.42	4.20	3.60	2.96	3.79	2.36	3.17

Table 4.16: G_{23} (GPa) for Different Combination of Flax and Jute Given in Table 4.10

Type of composite	Flax/epoxy	H1	H2	H3	H4	H5	Jute/epoxy
MSG	1.39	1.34	1.25	1.17	1.10	1.03	1.0
Modified Halpin-Tsai	1.43	1.38	1.29	1.21	1.13	1.05	1.02
% Diff (absolute)	2.79	2.89	3.10	3.31	2.65	1.90	1.96

Table 4.17: ν_{12} for Different Combination of Flax and Jute Given in Table 4.10

Type of composite	Flax/epoxy	H1	H2	H3	H4	H5	Jute/epoxy
MSG	0.398	0.396	0.391	0.385	0.380	0.374	0.371
RoHM	0.387	0.385	0.380	0.376	0.372	0.367	0.365
% Diff (absolute)	2.760	2.780	2.810	2.340	2.110	1.870	1.620

Table 4.18: ν_{13} for Different Combination of Flax and Jute Given in Table 4.10

Type of composite	Flax/epoxy	H1	H2	H3	H4	H5	Jute/epoxy
MSG	0.281	0.282	0.285	0.287	0.290	0.293	0.294
RoHM	0.293	0.294	0.295	0.296	0.297	0.299	0.299
% Diff (absolute)	4.096	4.082	3.389	3.041	2.357	2.007	1.672

Table 4.19: ν_{23} for Different Combination of Flax and Jute Given in Table 4.10

Type of composite	Flax/epoxy	H1	H2	H3	H4	H5	Jute/epoxy
MSG	0.441	0.439	0.433	0.0.426	0.420	0.413	0.411

Observation

– Flax/epoxy, jute/epoxy and flax/jute/epoxy lamina are orthotropic in nature.

– The flax/jute/epoxy hybrid composite has not showed any synergistic effect.

In the next chapter, synergistic effect, whether it is possible or not, if possible how much synergy is possible – will be described elaborately.

CHAPTER 5
SYNERGISTIC EFFECT DUE TO HYBRIDIZATION

5.1 Introduction

In this chapter, synergistic effect on longitudinal and transverse Young's moduli due to hybridization of natural fibers in the epoxy matrix is studied elaborately.

The upper and lower bounds for the effective stiffness of two phase composites have been studied for a long time. Among them, works of Voigt and Reuss are noteworthy. Voigt [W. Voigt, 1889] adopted isotrain assumption to obtain the estimation of the effective composite stiffness matrix as the weighted volume average of the stiffness matrices of constituent phases, while Reuss [A. Reuss, 1929] estimated the effective composite compliance matrix as the weighted volume average of the compliance matrices of constituent phases. In his work, Hill [35] showed that for isotropic constituent phases and composites, Voigt estimation provides the upper bounds and Reuss estimation provides the lower bounds for the effective bulk and shear moduli of composites.

In many text books and literatures, authors used two special composite layouts (serial connection as shown in figure 5.1 and parallel connection as shown in figure 5.2) to investigate the lower bound and upper bound of Young's modulus of composites. The constituent phases are isotropic elastic with Young's moduli E_A and E_B, volume fractions ϕ_A and ϕ_B, respectively.

By neglecting Poisson effects, the serial and parallel layouts are essentially one-dimensional models, and satisfy isostrain (Voigt) and isostress (Reuss) conditions. Therefore, the bounds for Young's modulus of the composite, $E_{composite}$ can be expressed as following based on Hill's work

$$\overline{E}_{Reuss} \leq E_{composite} \leq \overline{E}_{Voigt} \tag{5.1}$$

where

$$\overline{E}_{Voigt} = \phi_A E_A + \phi_B E_B \tag{5.2}$$

$$\overline{E}_{Reuss} = \frac{E_A E_B}{\phi_A E_B + \phi_B E_A} \tag{5.3}$$

Here, the overhead tildes in $\overline{E}_{Voigt}$ and $\overline{E}_{Reuss}$ mean that these effective moduli only approximately satisfy Voigt (isostrain) and Reuss (isostress) conditions due to neglecting Poisson effect.

Based on Equations 5.1-5.3, the following inequalities can be derived and have been widely considered to be valid for any situation [36].

Inequality I

$$E_{composite} \leq \overline{E}_{Voigt} = \phi_A E_A + \phi_B E_B \tag{5.4}$$

Equation 5.4 implies that $\overline{E}_{Voigt}$ can be used as the upper bound of the effective Young's modulus of the composite.

Inequality II

$$E_z^{eff} = E_{composite}^{serial} \leq E_{composite}^{parallel} = E_x^{eff} \tag{5.5}$$

Equation 5.5 implies that the longitudinal (or parallel) stiffness of a layered composite E_x^{eff} is always larger than the transverse (or serial) stiffness E_z^{eff}.

Inequality III

$$E_{composite} \leq max(E_A, E_B) \tag{5.6}$$

Equation 5.6 implies that the composite can not be stiffer than its stiffest constituent phase.

However, Poisson effect plays a vital role in the mechanical properties of composites and shouldn't be ignored. For example, Liu et. al. [37] found that the transverse stiffness of quasi-layered composites is significantly underestimated by the Reuss estimation. In this section effect of Poisson ratio on longitudinal stiffness (E_x^{eff}) and transverse stiffness (E_z^{eff}) of a two-phase layered composite is studied using three methods, namely, analytical method (developed by Liu et. al. [36]), FEM based MSG and classical lamination theory (CLT). Instead of using flax/epoxy lamina and jute/epoxy lamina, two isotropic phases, phase A and phase B are used to model the layered composite. For simplicity, it is assumed that the phases are isotropic in nature, with elastic moduli E_A and E_B, Poisson ratio ν_A and ν_B, volume fraction ϕ_A and ϕ_B. The laminate is made in A/B/A/B/A/B stacking sequence. This kind of laminate shows transverse isotropic behavior. If a composite laminate with stacking sequence of bFE/bJE/bFE/bJE/bFE/bJE is fabricated where bFE stands for bi-directional flax-epoxy and bJE stands for bi-directional jute-epoxy, it also shows transverse isotropy. That means such kind of laminate can effectively be represented using two-phase layered composite model.

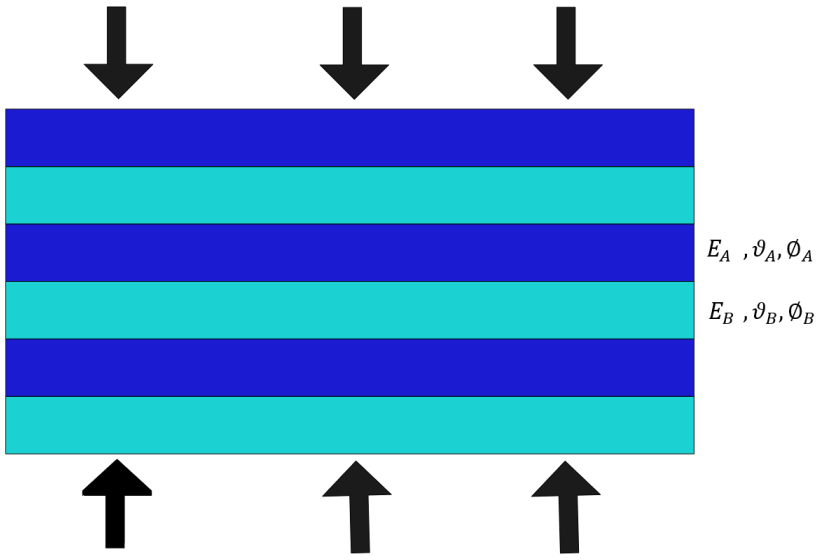

Fig. 5.1: A Schematic Diagram of a Layered Composite Under Transverse Compression (Serial Connection)

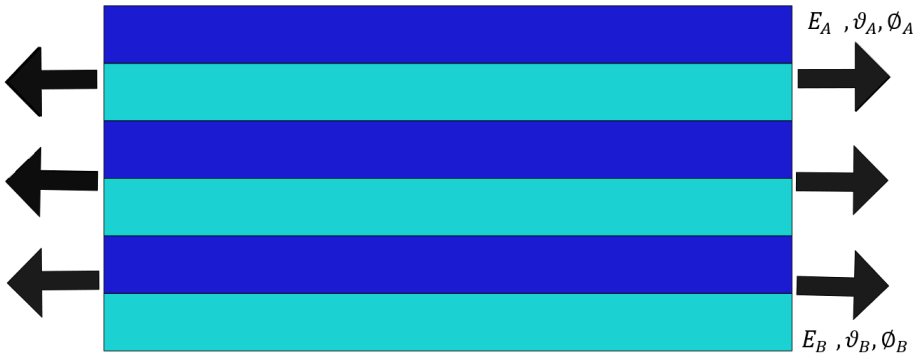

Fig. 5.2: A Schematic Diagram of a Layered Composite Under Longitudinal Tension (Parallel Connection)

Analytical Method

Bin Liu *et. al.* developed analytical equations for calculating longitudinal and transverse Young's modulus of a two-phase composite laminate [36].

$$E_x^{eff} = (\phi_A E_A + \phi_B E_B) + \frac{\phi_A \phi_B E_A E_B (\nu_A - \nu_B)^2}{\phi_A E_A (1 - \nu_B^2) + \phi_B E_B (1 - \nu_A^2)} \tag{5.7}$$

$$E_z^{eff} = \frac{E_A E_B}{\phi_A E_B + \phi_B E_A - \frac{2\phi_A \phi_B (\nu_A E_B - \nu_B E_A)^2}{(1-\nu_A)\phi_B E_B + (1-\nu_B)\phi_A E_A}} \tag{5.8}$$

Here,

E_A = Young's modulus of lamina A

E_B = Young's modulus of lamina B

ν_A = Poisson's ratio of lamina A

ν_B = Poisson's ratio of lamina B

ϕ_A = Volume fraction of lamina A

ϕ_B = Volume fraction of lamina B

E_x^{eff} = Longitudinal Young's modulus of two-phase composite

E_z^{eff} = Transverse Young's modulus of two-phase composite

FEA Based MSG Method

To investigate synergistic effect due to hybridization using FEA based MSG, an RVE like the one shown in Figure 5.3 has been used.

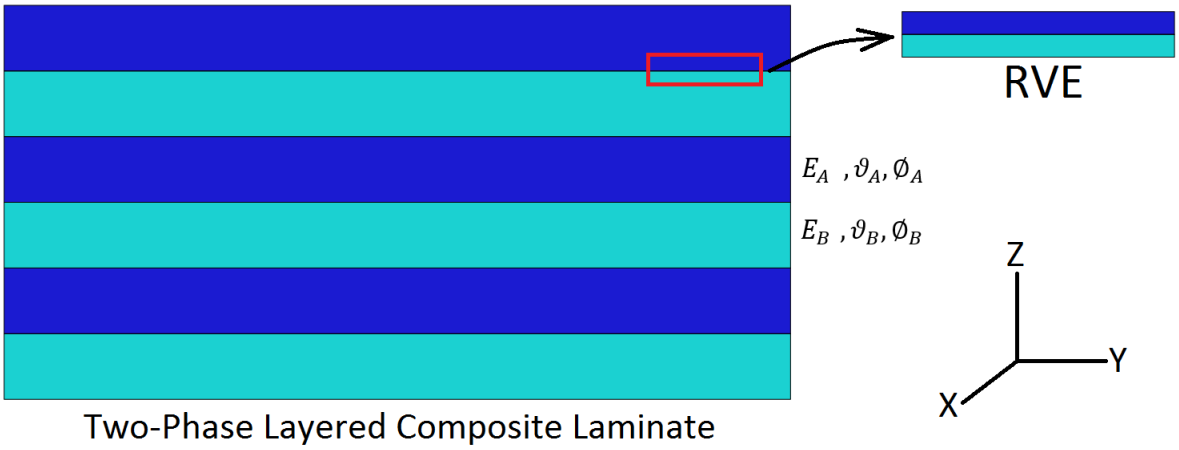

Fig. 5.3: Selection of RVE for FEA Analysis

Classical Lamination Theory (CLT)

Similar to Euler-Bernoulli beam theory and the plate theory, the classical lamination theory is only valid for thin laminates with small displacment in the transverse direction. It shares the same classical plate theory assumptions like following -

1. Normals remain straight (they do not bend).
2. Normals remain unstretched (they keep the same length).
3. Normals remain normal (they always make a right angle to the neutral plane).

In addition, perfect bonding between layers is assumed. The assumptions under perfect bonding are -

1. The bonding itself is infinitesimally small (there is no flaw or gap between layers).
2. The bonding is non-shear-deformable (no lamina can slip relative to another).
3. The strength of bonding is as strong as it needs to be (the laminate acts as a single lamina with special integrated properties).

For a two-phase laminate consisting of two isotropic lamina A and B (Figure 5.3),

$$\overline{E}_x^{eff} = \overline{E}_y^{eff} = \frac{h}{H} \frac{(\frac{E_A}{1-\nu_A^2} + \frac{E_B}{1-\nu_B^2})^2 - (\frac{\nu_A E_A}{1-\nu_A^2} + \frac{\nu_B E_B}{1-\nu_B^2})^2}{\frac{E_A}{1-\nu_A^2} + \frac{E_B}{1-\nu_B^2}} \tag{5.9}$$

where,

h = Thickness of each laminae

H = Thickness of the laminate

5.2 Results and Discussion

In this section, we use the above formulas for the effective moduli of layered composite to check if Inequalities 5.4-5.6 valid or not. Specially attention will be given to Inequality 5.6.

For a composite with the following set parameters: $\nu_A = 0.25$, $E_B/E_A = 0.5$, $\phi_A = \phi_B = 50\%$, normalized Young's moduli E_x^{eff}/E_A and E_z^{eff}/E_A are plotted in Figure 5.4 as a function of Poisson ratio of phase B, ν_B. It is found that when ν_B approaches 0.5, both E_x^{eff} and E_z^{eff} becomes larger than Voigt bound, $\overline{E}_{Voigt} = \phi_A E_A + \phi_B E_B$. Therefore the following conclusion can be adopted.

Conclusion 1. The approximate Voigt estimation is not always the upper bound of the Young's modulus of composites. In other words *Inequality I* may not be right.

Conclusion 2. The transverse Young's modulus, E_z^{eff} is not always smaller than the longitudinal Young' modulus, E_x^{eff}. In fact when ν_B approaches to 0.5, E_z^{eff} becomes larger than E_x^{eff}. In other words, *Inequality II* may be wrong.

To further investigate the validness of *Inequality III*, the following parameters are set:

$\nu_A = 0.25$, $E_B/E_A = 0.9$, $\phi_A = \phi_B = 50\%$ and normalized transverse Young's modulus E_z^{eff}/E_A is plotted as a function of ν_B in figure 5.5. It is found that the effective Young's modulus in transverse direction can exceed the maximum modulus of its constituents, when ν_B approaches to 0.5. Therefore we can draw the following conclusion.

Conclusion 3. The effective Young's modulus of composites is not always smaller than the maximum modulus of its constituents if the Poisson ratio is taken into account. In other words, *Inequality III* may not be right.

Conclusion 4. Synergistic effect due to hybridization does exist!

To investigate if synergistic effect is possible for E_x^{eff}, we have plotted normalized Young's modulus in longitudinal direction E_x^{eff}/E_A as a function of ν_B in Figure 5.6. The parameters are set as: $\nu_A = 0.25$, $E_B/E_A = 1.0$, $\phi_A = \phi_B = 50\%$. It is found that E_x^{eff} can be larger than the maximum value of Young's modulus of constituents A and B. That is why the following conclusion can be drawn.

Conclusion 5. Not only transverse Young's modulus, but also longitudinal Young's can be larger than Young's modulus of stiffest constituent of the composite. That means, E_x^{eff} can also show synergy. The more the difference between the Poisson ratio of the constituents, the more synergistic effect will be.

To investigate the effect of Young's modulus of individual phase on synergy, E_x^{eff} is plotted against varying Young's modulus of phase B, E_B in Figure 5.7 and 5.8. All the methods, namely, analytical, MSG and CLT have been used in calculating E_x^{eff}. The parameters are set at: $E_A = 50$, $\nu_A = 0.45$, $\nu_B = 0.15$ $\phi_A = \phi_B = 50\%$. It is found that the more the Young's moduli of two constituents approach to each other, the more synergy the composite shows.

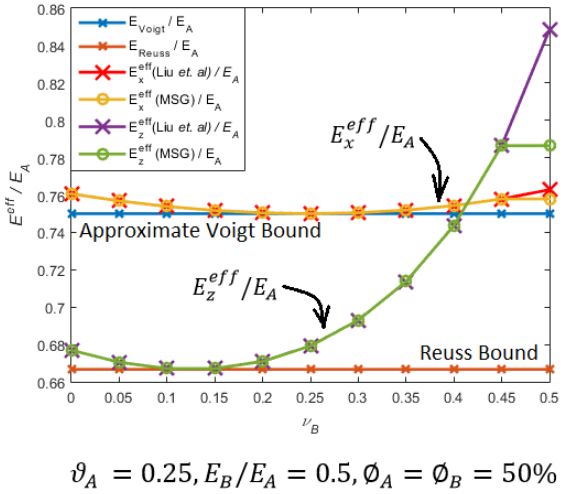

Fig. 5.4: The Normalized Effective Young's Moduli of the Layered Composite as a Function of the PoissonCHAR13s Ratio of Phase B

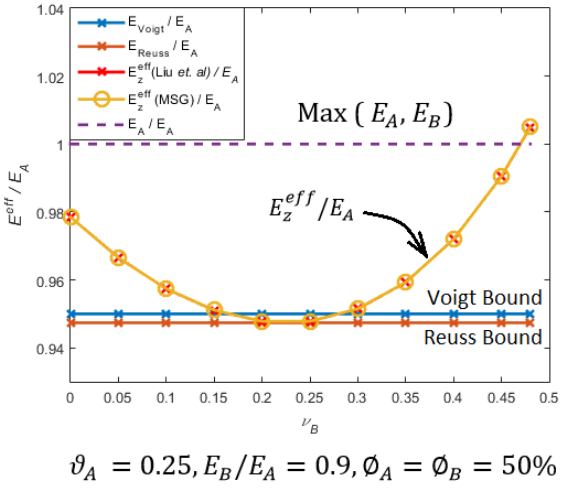

Fig. 5.5: The Normalized Effective Transverse Young's Modulus of the Layered Composite as a Function of the Poisson's Ratio of Phase B

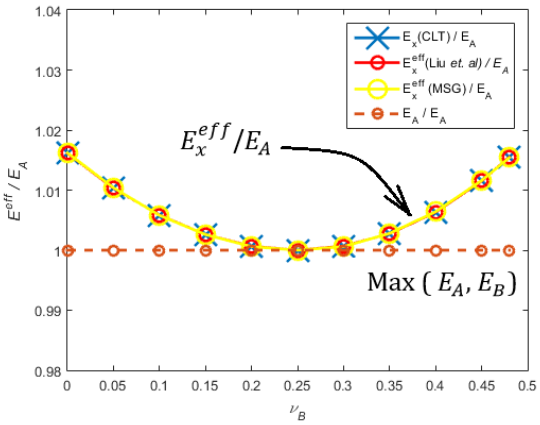

$\vartheta_A = 0.25, E_B/E_A = 1.0, \emptyset_A = \emptyset_B = 50\%$

Fig. 5.6: The Normalized Effective Longitudinal Young's Modulus of the Layered Composite as a Function of the Poisson's Ratio of Phase B

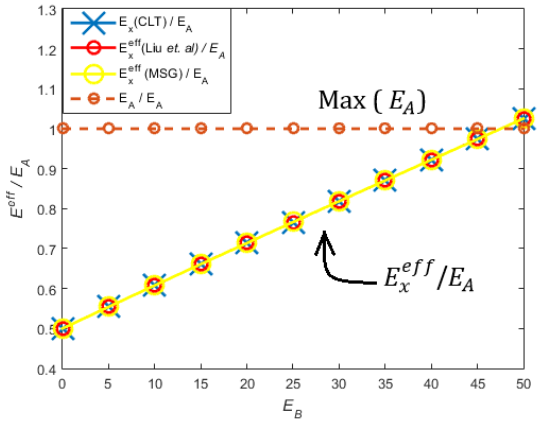

$E_A = 50, \vartheta_A = 0.45, \vartheta_B = 0.15, \emptyset_A = \emptyset_B = 50\%$

Fig. 5.7: The Normalized Effective Longitudinal Young's Modulus of the Layered Composite as a Function of the Young's Modulus of Phase B

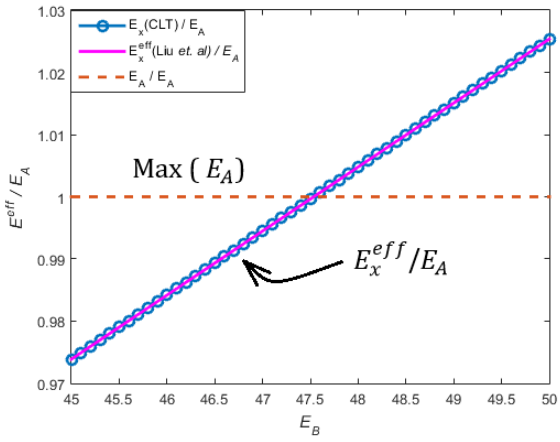

$E_A = 50, \vartheta_A = 0.45, \ \vartheta_B = 0.15, \emptyset_A = \emptyset_B = 50\%$

Fig. 5.8: The Normalized Effective Longitudinal Young's Modulus of the Layered Composite as a Function of the Young's Modulus of Phase B

5.3 Study of Synergistic Effect Due to Hybridization of Flax / Epoxy and Jute / Epoxy Given in Section 4.4

For 30% volume fraction of fiber, effective properties of unidirectional flax/epoxy and jute/epoxy are evaluated in section 4.4 and also given in Table 5.1. In this section composite laminates of unidirectional flax/epoxy and jute/epoxy are considered with fiber stacking sequence of $[0, \pm 60]_s$ (Figure 5.9). This kind of stacking sequence results in quasi isotropic laminate (isotropic in plane, but not isotropic out of plane). ABD matrix is evaluated using CLT. Equations used to evaluate ABD matrices can be found in any standard textbook. Now effective engineering properties of the quasi-isotropic laminate of flax/epoxy and jute/epoxy can be evaluated like following-

$$\overline{E}_x \equiv \frac{A_{11}A_{22} - A_{12}^2}{A_{22}H} \tag{5.10}$$

$$\overline{E}_y \equiv \frac{A_{11}A_{22} - A_{12}^2}{A_{11}H} \tag{5.11}$$

$$\overline{G}_{xy} \equiv \frac{A66}{H} \tag{5.12}$$

$$\overline{\nu}_{xy} \equiv \frac{A12}{A22} \tag{5.13}$$

$$\overline{\nu}_{yx} \equiv \frac{A12}{A11} \tag{5.14}$$

For quasi-isotropic laminate, $A_{11} = A_{22}$ and so

$$\overline{E}_x = \overline{E}_y \qquad \overline{\nu}_{xy} = \overline{\nu}_{yx} \tag{5.15}$$

Table 5.1: Effective Properties of Unidirectional Flax/Epoxy and Jute/Epoxy Calculated Using MSG with V_f=30%

Type of composite	E_1 (GPa)	E_2 (GPa)	ν_{12}	G_{12} (GPa)
Flax/epoxy	17.89	4.36	0.398	1.48
Jute/epoxy	15.31	3.76	0.371	1.27

For quasi-isotropic $[0, \pm 60]_s$ laminate of flax/epoxy and jute/epoxy, calculated effective properties using Equations 5.10-5.14 are given in Table 5.2.

Table 5.2: Effective Properties of Quasi-isotropic Flax/Epoxy and Jute/Epoxy Laminate

Type of composite	$\overline{E}_x$ (GPa)	$\overline{E}_y$ (GPa)	$\overline{\nu}_{xy}$	$\overline{G}_{xy}$ (GPa)
Quasi-isotropic flax/epoxy	8.62	8.62	0.355	3.18
Quasi-isotropic jute/epoxy	7.39	7.39	0.347	2.74

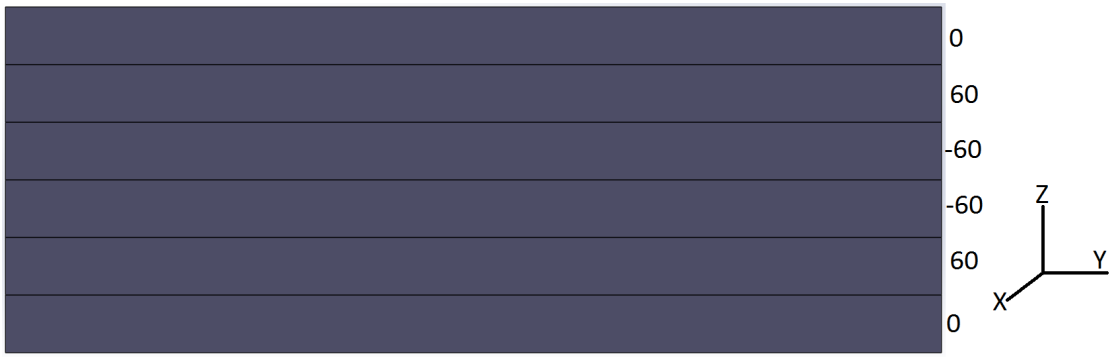

Fig. 5.9: Quasi-isotropic Laminate

Now a new laminate consisting of quasi-isotropic flax/epoxy (qFE) and quasi-isotropic jute/epoxy (qJE) is modeled. Even though any of the two stacking sequences - $[qFE(0^o)/qJE(0^o)]_T$ or $[qFE(0^o)/qJE(0^o)]_s$ - could be used, the later one, that is $[qFE(0^o)/qJE(0^o)]_s$ is used here, because it is recommended to use symmetric laminate to calculate effective properties using CLT [Hyer]. The calculated effective engineering properties of the hybrid qFE/qJE are given in Table 5.3.

Table 5.3: Effective Properties of Hybrid Laminate (qFE/qJE)

Type of composite	$\overline{E}_x$ (GPa)	$\overline{E}_y$ (GPa)	$\overline{\nu}_{xy}$	$\overline{G}_{xy}$ (GPa)
qFE	8.62	8.62	0.355	3.18
qJE	7.39	7.39	0.347	2.74
qFE/qJE	8.01	8.01	0.351	2.96

Conclusion 1. Synergistic effect is not available. It may be because the ratio of Young's moduli of qJE to qFE is 0.86. But to get synergistic effect, according to Figure 5.8, the ratio of Young's between two phases needs to be more than 0.94. That means to get synergistic effect, Young's moduli of qFE and qJE need to be closer.

Conclusion 2. From Figure 5.6, we see that the more the difference between Poisson ratio of two phases, the more synergistic effect will be. From Table 5.3, we see that Poisson ration of qFE and qJE are pretty close. The greater the difference will be, the greater the chance of getting synergy will be.

To study if the angle difference between the layers of flax/jute/epoxy hybrid composite material produces any kind of synergistic effect in the effective Young's modulus of the hybrid, a hybrid composite material with stacking sequence of JE(30^o)/FE(θ)/FE(θ)/JE(30^o) is studied using classical lamination theory, where JE stands for jute/epoxy and FE stands for flax/epoxy. The angle of JE laminae is kept fixed at 30^o, while the angle of FE laminae is varied from $\theta = 90^o$ to $\theta = -90^o$. No synergistic effect is found, from which it is concluded that Poisson ratio difference between the layers is the main driving factor to produce synergistic effect in hybrid composite laminate.

CHAPTER 6

IMPACT PROPERTIES OF FLAX/JUTE/EPOXY HYBRID COMPOSITE

6.1 Introduction

In the previous chapter we showed that synergistic effect in Young's modulus due to hybridization of two different fibers in the same matrix is possible. To show it, we used two isotropic phases of materials. The two phases represented flax/epoxy laminae and jute/epoxy laminae, respectively. Resulting two phase layered composite was a transversely isotropic material. This kind of transverse isotropy can be achieved by using bidirectional weaves of fibers embedded in a matrix material. On the other hand, quasi-isotropy can be achieved by using fiber blends mixed with matrix material. In literature, most of the authors used either bi-directional hybrid composites or fiber blends mixed with matrix material, for example in [38], [39] and [40]. In this chapter, Charpy impact testing of flax/jute/epoxy hybrid composite material has been described elaborately. Both of the fibers are bi-directional mats.

6.2 Materials and Processing

6.2.1 Fibers and Matrix

The fibers used here are jute plain weave and flax twill weave. Both of them have been collected from easycomposites, UK. The epoxy resin system used in this study is PT2050 and hardener is B1, both of them collected from PTMW industries. The resin and hardener are mixed in 100:27 proportion according to the manufacturer's specification. Table 6.1 presents some of the properties of fibers and matrix according to manufacturer's specification being used here.

Table 6.1: Density and Modulus of Fiber and Matrix Used in this Study

Type of composite	Density (g/cm^3)	Modulus (GPa)
Flax Fiber	1.50	50
Jute Fiber	1.46	40
Epoxy Resin	1.1	3

Epoxy as a Matrix

The manufacture of natural fiber composites includes the use of either a thermoplastic polymer or a thermoset polymer binder system combined with the natural fiber. Among thermoplastic polymers, polypropylene, polyethylene, polystyrene and polyamides are noteworthy. On the other hand, polyester, vinylester and epoxy are some of the mostly used thermoset polymers. Thermoplastic polymers are mainly used for nonstructural applications, while thermoset polymers are good for structural applications. Choice of matrix material depends on two main factors.

1. Melting Temperature :

Melting temperature (T_m) of most of the thermoplastic polymers is on the order of 120 C. On the other hand, for natural fibers, the upper limit before fiber degradation occurs is on the order of 150 C for long processing durations. Fiber can withstand as much as 220 C for short-term exposure. That means even though fibers have a higher range of temperature endurance, they are forced to be used at a lower temperature (lower than 120 C) due to the fact that thermoplastic resin to be used as the binder can't withstand a higher temperature. Thermoset polymers like epoxy are free from such kind of temperature restriction.

2. Difference in Surface Energy :

The difference between the surface energy of natural fibers and polymer matrix determines the strength between the filler and the binder. The less the difference is, the stronger the bond between the filler and the binder will be.

The excellent adhesive properties of epoxy resins are due to the attractive forces between the epoxy resin and the surface of the fiber. These forces are usually polar forces or direct bonds that can perform between reactive sites in the resin and reactive or polar sites on the surface of the fiber. Typical epoxy resins have hydroxyl (OH^-) groups along their chain which can form bonds or strong polar attractions to oxide or hydroxyl surfaces. In natural fibers, polar groups emanate from hydroxyl groups, acetyl and ether linkages ($C-O-C$). Polar groups coming from natural fibers make strong bonds with hydroxyl groups coming from epoxy. As both of the filler and the binder have polarity on the surface, they have very high yet close to each other surface energy, which ensures strong bond between them. That's why, natural fiber composites with epoxy as a matrix material show superior mechanical properties.

An important advantage of epoxy resin that also makes them good adhesives is that they do not need anything other than the chemicals themselves to cause the cure. Some adhesives only cure in the absence of air, some only cure in the presence of moisture or humidity. Epoxy glues cure by themselves without any other material being needed. The versatility of epoxies is also an advantage in considering them for adhesive applications. A list of attractive features of epoxy as a matrix material is given below.

- They can cure at room temperature
- They can be heat-cured to provide a high service temperature for the adhesives
- They can be supplied as a one-part adhesive that does not require any mixing
- They can be supplied in flexible or rigid forms to match their cured state properties to the stresses they will be exposed to
- They can be cured underwater

6.2.2 Processing Setup

Five different hybridized composites with varying flax fiber volume fractions were manufactured. The volume fraction of flax and jute in different samples are showed in Table 6.2. Fiber volume fractions were controlled by increasing or decreasing the amount of flax or jute fiber plies. The fiber layering sequence was held constant for all hybridized compos-

ites. The fiber layering sequence was [Flax/Jute/Flax/Jute/Flax]. The fibers were evenly distributed so that a symmetric and balanced laminate was produced. The ply stacking configurations for the various processed panels are given in Table 6.3.

All additional flax fiber plies were added to the center of the laminate. Due to higher tensile strength of flax fiber compared to jute fiber, adding extra flax fibers to the outermost regions of the laminate would drastically increase the flexural strength. To help isolate the effects of varying the fiber volume fraction of the fibers, additional fiber layers were applied as close to the laminate's neutral axis as possible, where normal stresses approach zero.

Prior to infusion, fiber mats were cut into small pieces with equal dimensions. Vacuum assisted resin transfer molding (VARTM) method was implemented to manufacture all the composites used in this study. After the VARTM set-up was made ready, epoxy was infused into the fibers by using rollers and brush (hand lay up). Once the infusion process was complete, the laminate was placed into VARTM setup under negative pressure for 12 hours. After 12 hours, the laminate was removed from the processing table and kept in room temperature for at least 24 hours for post curing. Composite manufacturing process using VARTM is showed in Figure 6.1.

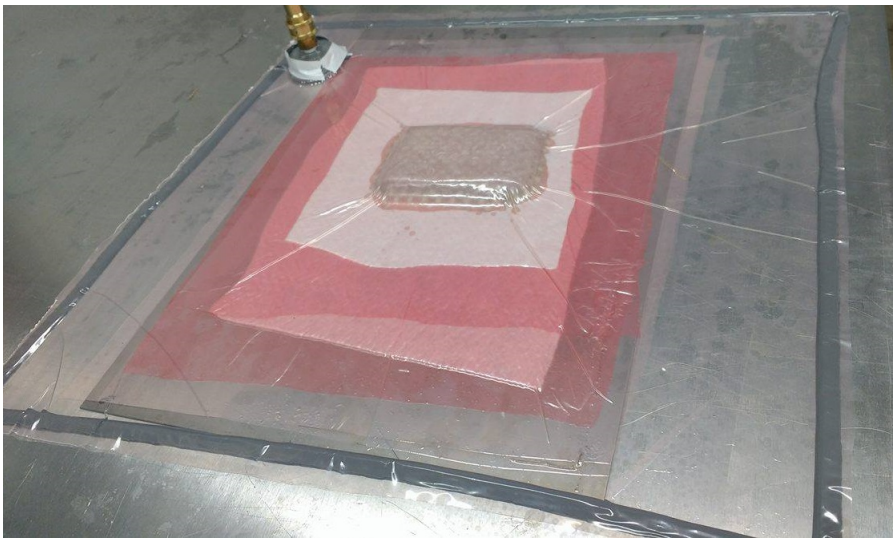

Fig. 6.1: Vacuum Assisted Resin transfer Method (VARTM)

Table 6.2: Combination of flax and jute

Specimen	$V_F(\%)$	$V_J(\%)$	$V_f(\%)$
H1	0	30	30
H2	12.94	17.06	30
H3	20.60	9.40	30
H4	25.76	4.24	30
H5	30	0	30

Table 6.3: Processed Panels Ply Stacking Order

Panel Configuration	Flax Plies	Jute Plies	Flax Plies	Jute Plies	Flax Plies	Fiber Volume Fraction (Flax/Jute)
Only Flax	-	-	-	-	-	30/0
1	2	1	7	1	2	25.76/4.24
2	2	3	4	3	2	20.60/9.40
3	2	5	1	5	2	12.94/17.06
Only Jute	-	-	-	-	-	0/30

6.3 Impact Testing

Using Izod impact test method to determine impact strength of composites is strongly discouraged in ASTM D256 test procedure. The reason behind is that such kind of test specimen may be seriously affected by interface effects or effects of solvents and cements on energy absorption of test specimens, or both. That is why here Charpy impact testing

according to ASTM D6110 is followed. Even though ASTM D6110 is originally designed for notched specimens of plastics, due to unavailability of any ASTM standards for Charpy impact testing of composites, ASTM D6110 has been modified here to accomodate composite materials.

Charpy impact test can be performed on either notched or unnotched specimens. A notched specimen is used to predefine the crack direction, while an unnotched specimen is used to study the mode of fracture. In this study notched specimens were used. The impact blow can be in either the edgewise or the flatwise direction for most of the materials as showed in Figures 6.2, 6.3. Choosing a direction of blow depends on the purpose of the testing. To study the impact strength of the surface of composite samples, flatwise impact blow is used. On the other contrary, to study the delamination process of the samples, edgewise impact blow is used. In the current study, flatwise impact blow was used.

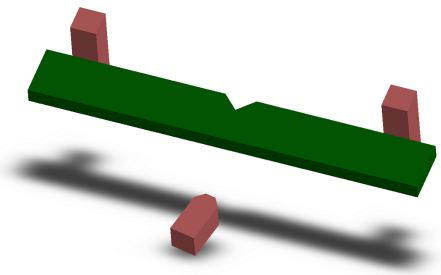

Fig. 6.2: Edgewise Impact Blow

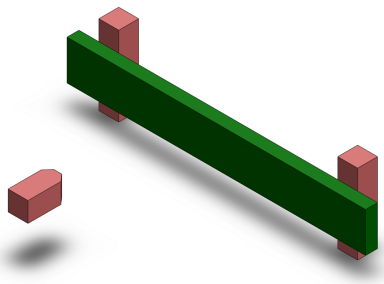

Fig. 6.3: Flatwise Impact Blow

For the impact study, Tinius Olsen Impact Tester Model 892 was used. The tester has the following weight configurations.

ASTM configuration

→ No weights will give a capacity of 25 in-lbs

→ Weights marked as 2017 will give a capacity of 50 in-lbs

→ Weights marked as 2018 will give a capacity of 100 in-lbs

→ Weights marked as 2019 will give a capacity of 200 in-lbs

ISO configuration

→ No weights will give a capacity of 2.8 J

→ Weights marked as 2022 will give a capacity of 5.0 J

→ Weights marked as 2023 will give a capacity of 7.5 J

→Weights marked as 2024 will give a capacity of 15 J

→ Weights marked as 2025 will give a capacity of 25 J

Even though weights marked as 2023 are suitable for ISO standards, those were used for the study carried out here according to ASTM D6110, due to the unavailability of the other weights compatible for ASTM configuration. After adding new weights, weight input was updated in the Tinius Olsen Impact Tester. The process of how to change the weight input is well described in the manual. After adding the new weights, calibration was done. Before each of the impact tests, the machine was recalibrated to ensure that the machine was showing correct potential energy. Each time the machine was showing 7.5 ± 0.15 J, which is very close to the set value of 7.5J. In ASTM D6110, complete break of specimen is recommended. During the current study, each specimen broke completely conforming to the ASTM standard. For each panel configuration, at least 5 specimens were used and the average value was calculated. The dimensions of the samples were 125×10×12.7 mm as shown in Figure 6.4. Noteworthy that, maintaining a height of 12.7mm and at the same time maintaining specific panel configuration as showed in Table 6.3 were difficult. To remove meniscus formed on the samples, they were sanded properly before doing the experiment. A sample before sanding and after sanding is shown in Figures 6.5 and 6.6.

Results and Discussion

Results of Charpy impact test can be found in Figures 6.7, 6.8 and Table 6.4. The results are showed both in terms of impact strength (kJ/m^2) and break energy (J). Impact strength of jute/epoxy is $33.54kJ/m^2$, while impact strength of flax/epoxy is $44.09kJ/m^2$. That means impact strength of falx/epoxy is 23.93% larger than jute/epoxy. So by introducing flax into jute/epoxy, impact strength can significantly be increased, while due to the lower weight of jute, the lightness of the structure can still be maintained.

The failure of the samples is mainly due to fiber breaking. That is why, due to higher mechanical properties of flax fiber, with the increase of flax fiber, impact strength increases. At 25.76% volume fraction of flax, the impact strength of the hybrid composite increases in such a way that it surpasses the impact strength of flax/epoxy composite sample. Even though the increase is very small, the reason for this increase in impact strength can be seen in the mixture of failure modes that occur during impact. In addition to fiber breaking, the failure results from fiber pull-out. Figure 6.9 shows a microscopic image of flax/epoxy and Figure 6.10 shows a microscopic image of flax/jute/epoxy where volume fraction of flax is 25.76%. In case of flax/epoxy, the failure comes from fiber breaking only. But in case of flax/jute/epoxy with 25.76% of flax, the failure comes from both fiber breaking and fiber pull-out. Due to incorporation of two types of failure modes in flax/jute/epoxy hybrid composite, break energy as well as impact strength increase and surpass the break energy and impact strength of flax/epoxy. Such kind of increase is not uncommon. Researchers have found that incorporating small percentages of low-modulus but high strength fibers is an effective means of increasing the impact performance of composites [41]. Finally, Figure 6.11 demonstrates the percent increase in impact strength with incorporation of flax fiber in the jute/epoxy composite.

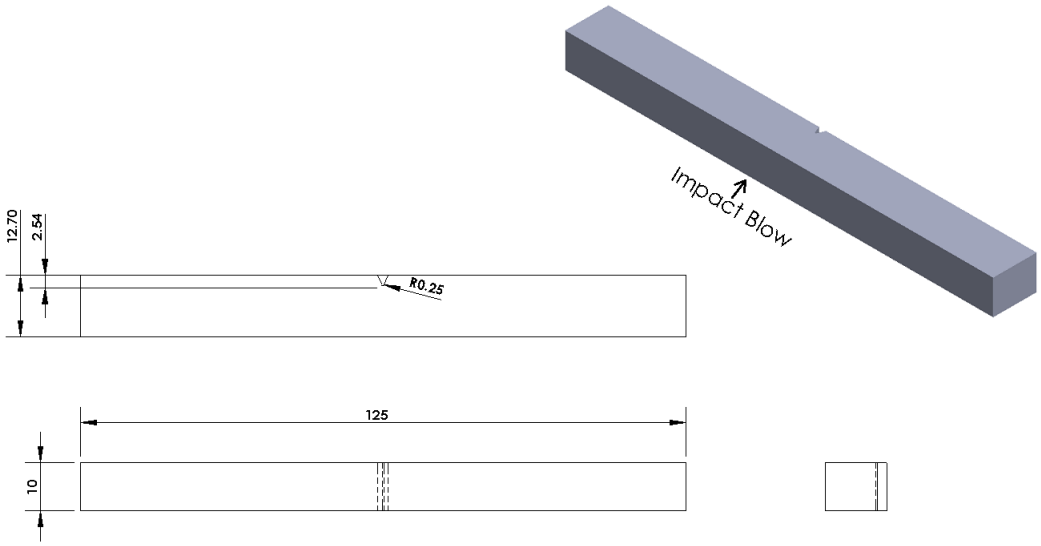

Fig. 6.4: Dimension of the Specimen

Fig. 6.5: Composite Sample Before Sanding

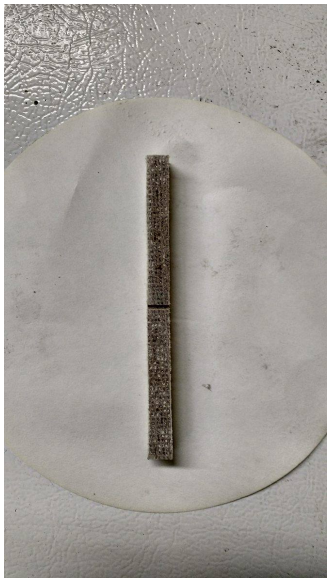

Fig. 6.6: Composite Sample After Sanding

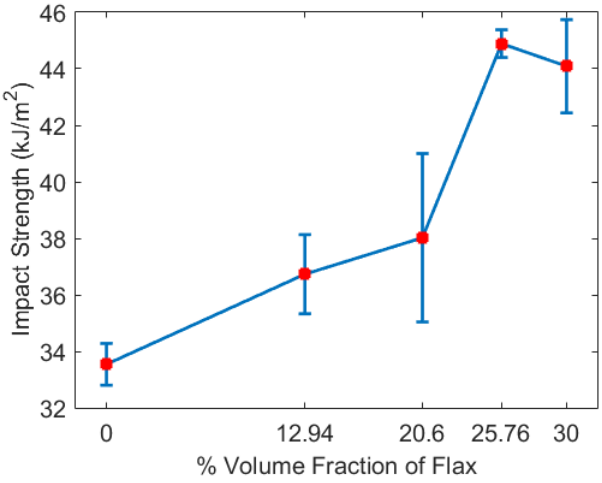

Fig. 6.7: Impact Strength Versus Flax Fiber Loading Results from Charpy Impact Testing

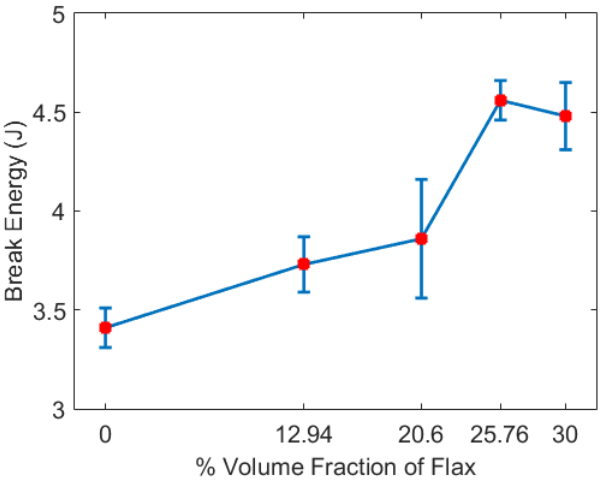

Fig. 6.8: Break Energy Versus Flax Fiber Loading Results from Charpy Impact Testing

Fig. 6.9: Microscopic Image of Surface Morphology After Impact Failure of Flax/Epoxy Composite

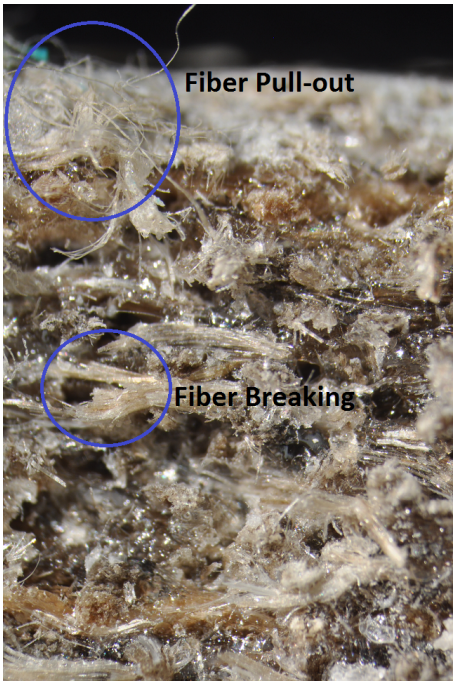

Fig. 6.10: Microscopic Image of Surface Morphology After Impact Failure of Flax/Jute/Epoxy Composite ($V_{flax} = 25.76\%$)

Table 6.4: Results From Charpy Impact Testing

Panel Configuration	Width (mm)	Break Energy (J)	Impact Strength (kJ/m^2)	Values from Literature
Flax/Epoxy	10	4.48	44.09	38.4 kJ/m^2 [41]
1	10	4.56	44.89	-
1	10	3.86	38.02	-
3	10	3.73	36.73	-
Jute/Epoxy	10	3.41	33.54	3.44J [42]

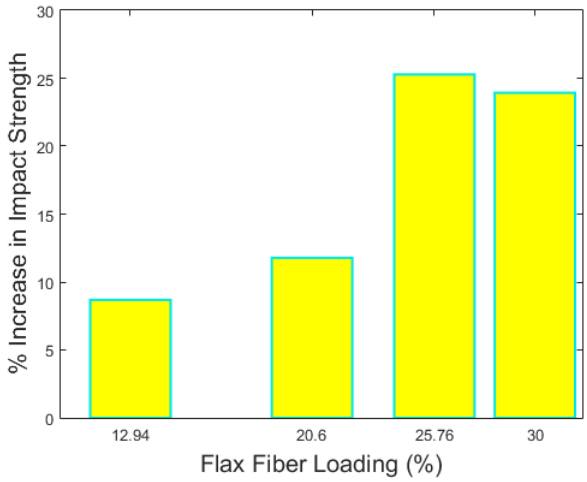

Fig. 6.11: Percent Increase in Impact Strength with Increase of Flax Fiber Loading (Total Fiber Volume Fraction is Fixed at 30%)

CHAPTER 7
SUMMARY, CONCLUSION, AND FUTURE WORK

7.1 Summary of Work Performed

As a part of this thesis, the microstructure of flax fiber and jute fiber is studied using scanning electron microscopy (SEM). It's found that the cross sections of flax fiber and jute fiber are polygonal. Flax fiber has either very small hole (lumen) or no hole at all. On the other hand, jute fiber has a relatively bigger hole at the center of the fiber cell.

Cell wall of natural fibers consists of five layers mainly, M, P, S1, S2, S3. S1, S2, and S3 together are called secondary layer. Due to the large thickness and cellulose alignment, S2 controls the mechanical properties of natural fibers. That's why, it is assumed that cell walls of flax and jute consist of S2 layer only with a lumen at the center. This kind of assumption simplifies the analysis greatly without compromising the accuracy of the results. Effective mechanical properties of flax and jute fibers are calculated in two steps. In the first step, effective mechanical properties of S2 layers of flax and jute are calculated numerically and validated analytically. In the second step, effective mechanical properties of flax fiber and jute fiber are calculated numerically. After calculating the effective mechanical properties of flax fiber and jute fiber, effective mechanical properties of flax/jute/epoxy hybrid composite are calculated numerically and compared with analytical results. The overall volume fraction of fiber is kept fixed at 30%, while the relative volume fraction of flax and jute are changed to see the effect of them on the mechanical properties of the hybrid composite material.

To study the synergistic effect due to the hybridization of two natural fibers in the epoxy matrix, two phased layered composite is considered. One phase corresponds to flax/epoxy laminae while the other phase corresponds to jute/epoxy laminae. Each phase is isotropic in nature. This kind of two phased layered composite results in transversely isotropic behavior.

If a composite laminate with stacking sequence of bFE/bJE/bFE/bJE/
bFE/bJE is fabricated where bFE stands for bidirectional flax-epoxy and bJE stands for bi-directional jute-epoxy, it also shows transverse isotropy. That means such kind of laminate can effectively be represented using two-phase layered composite model.

Finally, impact properties of flax/epoxy, jute/epoxy, and flax/jute/epoxy hybrid composite materials are studied using Charpy impact testing. The overall fiber volume fraction is kept fixed at 30%, while the relative volume fraction of flax and jute is changed gradually. For each combination of flax and jute, at least five samples are tested.

7.2 Summary of Findings and Conclusion

Microstructure of Flax and Jute

1. Both flax and jute have polygonal cross section.

2. Flax either has no lumen, or very small one, if any. On the other hand, jute has a relatively bigger lumen at the center of the fiber.

Numerical Modeling

1. S2 layers of both flax and jute exhibit transversely isotropic behavior. Longitudinal elastic modulus of S2 layer of flax is larger than the longitudinal elastic modulus of S2 layer of jute. It's because the cellulose content in the S2 layer of flax is more than the cellulose content in the S2 layer of jute.

2. Flax fiber and jute fiber exhibit orthotropic behavior. Longitudinal elastic modulus of flax fiber is larger than the longitudinal elastic modulus of jute fiber. It's because S2 layer of flax fiber has a larger longitudinal elastic modulus value than that of jute fiber. In addition, the lumen of flax is smaller compared to the lumen of jute.

3. As cellulose is the stiffest among all the three constituents, with the increase of volume fraction of cellulose in S2 layer of flax and jute, stiffness increases.

4. Cellulose angel in flax fiber varies from 6^o to 10^o. With the increase of cellulose angle with the fiber axis, longitudinal elastic modulus value decreases.

5. Flax/epoxy, jute/epoxy, flax/jute/epoxy - all of them show orthotropic mechanical behavior. As flax is stiffer than jute, with the increase of relative volume fraction of flax fiber

in flax/jute/epoxy hybrid composite material, stiffness of the hybrid composite increases.

Synergistic Effect Due to Hybridization

1. The approximate Voigt estimation is not always the upper bound when the Poisson ratio of the constituents is taken into consideration.

2. The transverse Young's modulus is not always smaller than the longitudinal Young's modulus. In fact it can be larger than the longitudinal Young's modulus when Poisson ratio is taken into consideration.

3. The effective Young's modulus of composites is not always smaller than the maximum modulus of its constituents if the Poisson ratio is taken into account. That means synergistic effect exists, and it occurs due to the Poisson ratio difference between the constituents. For example, due to the difference of Poisson ratio between the flax/epoxy laminae and the jute/epoxy laminae, flax/jute/epoxy hybrid laminate can show effective Young's modulus larger than effective Young's modulus of both flax/epoxy and jute/epoxy.

4. Both longitudinal Young's modulus and transverse Young's modulus of the hybrid composite can be larger than the Young's modulus of the stiffest constituent of the composite.

5. The more the difference between the Poisson ratio of the constituents, the more synergistic effect the hybrid composite will show. For example, the more the difference in Poisson ratio between the flax/epoxy laminae and jute/epoxy laminae, the more synergistic effect the flax/jute/epoxy hybrid laminate will show. However, this synergy beyond upper bound seems to be small.

Charpy Impact Testing

1. Flax/epoxy has a larger impact strength than jute/epoxy.

2. When a small amount of jute is introduced in flax/epoxy, the new flax/jute/epoxy hybrid composite shows larger impact strength than flax/epoxy itself. That means, flax/jute/epoxy shows synergistic effect. Such kind of increase is not uncommon. Researchers have found that incorporating small percentages of low-modulus but high strength fibers is an effective means of increasing the impact performance of composites. In case of flax/epoxy, the impact

failure occurs from fiber breaking only. But when a small amount of jute is incorporated, the failure occurs from both fiber breaking and fiber pull-out. Due to the incorporation of two modes of failure, impact strength of flax/jute/epoxy becomes larger than that of flax/epoxy composite material.

7.3 Future Work

The following tasks can be done in future -

1. Experimental testing of flax fiber and jute fiber can help to validate the numerical results.

2. Tensile testing of flax/epoxy, jute/epoxy, and flax/jute/epoxy can help compare the experimental results with the numerical results.

3. Flexural testing can help to study the flexural strength of the composite materials.

4. Synergistic effect due to hybridization of flax fiber and jute fiber in epoxy can be studied experimentally.

5. Detailed SEM study after failure can help understand the failure mode of the composite materials.

REFERENCES

[1] Qing, H. and Jr., L. M., "3D hierarchical computational model of wood as a cellular material with fibril reinforced, heterogeneous multiple layers," *Mechanics of Materials*, Vol. 41, No. 9, 2009, pp. 1034 – 1049.

[2] Gassan, J., Chate, A., and Bledzki, A. K., "Calculation of elastic properties of natural fibers," *Journal of Materials Science*, Vol. 36, No. 15, 2001, pp. 3715–3720.

[3] Mohanty, A. K., Misra, M., and Hinrichsen, G., "Biofibres, biodegradable polymers and biocomposites: An overview," *Macromolecular Materials and Engineering*, Vol. 276-277, No. 1, 2000, pp. 1–24.

[4] Nickel, J. and Riedel, U., "Activities in biocomposites," *Materials Today*, Vol. 6, No. 4, 2003, pp. 44 – 48.

[5] O'Donnell, A., Dweib, M., and Wool, R., "Natural fiber composites with plant oil-based resin," *Composites Science and Technology*, Vol. 64, No. 9, 2004, pp. 1135 – 1145.

[6] Shibata, M., Ozawa, K., Teramoto, N., Yosomiya, R., and Takeishi, H., "Biocomposites Made from Short Abaca Fiber and Biodegradable Polyesters," *Macromolecular Materials and Engineering*, Vol. 288, No. 1, 2003, pp. 35–43.

[7] Morye, S. and Wool, R., "Mechanical properties of glass/flax hybrid composites based on a novel modified soybean oil matrix material," *Polymer Composites*, Vol. 26, No. 4, 2005, pp. 407–416.

[8] Bodros, E., Pillin, I., Montrelay, N., and Baley, C., "Could biopolymers reinforced by randomly scattered flax fibre be used in structural applications?" *Composites Science and Technology*, Vol. 67, No. 34, 2007, pp. 462 – 470.

[9] Jawaid, M. and Khalil, H. A., "Cellulosic/synthetic fibre reinforced polymer hybrid composites: A review," *Carbohydrate Polymers*, Vol. 86, No. 1, 2011, pp. 1 – 18.

[10] Thwe, M. M. and Liao, K., "Durability of bamboo-glass fiber reinforced polymer matrix hybrid composites," *Composites Science and Technology*, Vol. 63, No. 34, 2003, pp. 375 – 387.

[11] Fu, S.-Y., Xu, G., and Mai, Y.-W., "On the elastic modulus of hybrid particle/short-fiber/polymer composites," *Composites Part B: Engineering*, Vol. 33, No. 4, 2002, pp. 291 – 299.

[12] John, M. J., Francis, B., Varughese, K., and Thomas, S., "Effect of chemical modification on properties of hybrid fiber biocomposites," *Composites Part A: Applied Science and Manufacturing*, Vol. 39, No. 2, 2008, pp. 352 – 363.

[13] Sreekala, M., George, J., Kumaran, M., and Thomas, S., "The mechanical performance of hybrid phenol-formaldehyde-based composites reinforced with glass and oil palm fibres," *Composites Science and Technology*, Vol. 62, No. 3, 2002, pp. 339 – 353.

[14] Joshi, S., Drzal, L., Mohanty, A., and Arora, S., "Are natural fiber composites environmentally superior to glass fiber reinforced composites?" *Composites Part A: Applied Science and Manufacturing*, Vol. 35, No. 3, 2004, pp. 371 – 376, {AIChE} 2002.

[15] Thomas, S., Idicula, M., and Joseph, K., "Mechanical performance of short banana/sisal hybrid fibre reinforced polyester composites," *Journal of Reinforced Plastics and Composites*, 2009.

[16] Jacob, M., Thomas, S., and Varughese, K., "Mechanical properties of sisal/oil palm hybrid fiber reinforced natural rubber composites," *Composites Science and Technology*, Vol. 64, No. 78, 2004, pp. 955 – 965.

[17] Jacob, M., Thomas, S., and Varughese, K. T., "Natural rubber composites reinforced with sisal/oil palm hybrid fibers: Tensile and cure characteristics," *Journal of Applied Polymer Science*, Vol. 93, No. 5, 2004, pp. 2305–2312.

[18] Jacob, M., Francis, B., Thomas, S., and Varughese, K., "Dynamical mechanical analysis of sisal/oil palm hybrid fiber-reinforced natural rubber composites," *Polymer Composites*, Vol. 27, No. 6, 2006, pp. 671–680.

[19] Jawaid, M., Khalil, H. A., and Bakar, A. A., "Mechanical performance of oil palm empty fruit bunches/jute fibres reinforced epoxy hybrid composites," *Materials Science and Engineering: A*, Vol. 527, No. 2930, 2010, pp. 7944 – 7949.

[20] Shinoj, S., Visvanathan, R., Panigrahi, S., and Kochubabu, M., "Oil palm fiber (OPF) and its composites: A review," *Industrial Crops and Products*, Vol. 33, No. 1, 2011, pp. 7 – 22.

[21] John, M. J. and Thomas, S., "Biofibres and biocomposites," *Carbohydrate Polymers*, Vol. 71, No. 3, 2008, pp. 343 – 364.

[22] Banerjee, S. and Sankar, B. V., "Mechanical properties of hybrid composites using finite element method based micromechanics," *Composites Part B: Engineering*, Vol. 58, 2014, pp. 318 – 327.

[23] Dong, C., Ranaweera-Jayawardena, H. A., and Davies, I. J., "Flexural properties of hybrid composites reinforced by S-2 glass and {T700S} carbon fibres," *Composites Part B: Engineering*, Vol. 43, No. 2, 2012, pp. 573 – 581.

[24] Song, J. H., "Pairing effect and tensile properties of laminated high-performance hybrid composites prepared using carbon/glass and carbon/aramid fibers," *Composites Part B: Engineering*, Vol. 79, 2015, pp. 61 – 66.

[25] de Medeiros, E. S., Agnelli, J. A. M., Joseph, K., de Carvalho, L. H., and Mattoso, L. H., "Mechanical properties of phenolic composites reinforced with jute/cotton hybrid fabrics," *Polymer Composites*, Vol. 26, No. 1, 2005, pp. 1–11.

[26] Marom, G., Fischer, S., Tuler, F. R., and Wagner, H. D., "Hybrid effects in composites: conditions for positive or negative effects versus rule-of-mixtures behaviour," *Journal of Materials Science*, Vol. 13, No. 7, 1978, pp. 1419–1426.

[27] Yu, W., "An Introduction to Micromechanics," *Composite Materials and Structures in Aerospace Engineering*, Vol. 828 of *Applied Mechanics and Materials*, Trans Tech Publications, 4 2016, pp. 3–24.

[28] Sun, C. and Vaidya, R., "Prediction of composite properties from a representative volume element," *Composites Science and Technology*, Vol. 56, No. 2, 1996, pp. 171 – 179.

[29] Sun, Z., Zhao, X., Wang, X., and Ma, J., "Multiscale modeling of the elastic properties of natural fibers based on a generalized method of cells and laminate analogy approach," *Cellulose*, Vol. 21, No. 3, 2014, pp. 1135–1141.

[30] Yu, W., "SwiftComp," Aug 2016.

[31] Charlet, K., Baley, C., Morvan, C., Jernot, J., Gomina, M., and Brard, J., "Characteristics of Herms flax fibres as a function of their location in the stem and properties of the derived unidirectional composites," *Composites Part A: Applied Science and Manufacturing*, Vol. 38, No. 8, 2007, pp. 1912 – 1921.

[32] Astley, R. J., Stol, K. A., and Harrington, J. J., "Modelling the elastic properties of softwood," *Holz als Roh- und Werkstoff*, Vol. 56, No. 1, 1998, pp. 43–50.

[33] Affdl, J. C. H. and Kardos, J. L., "The Halpin-Tsai equations: A review," *Polymer Engineering & Science*, Vol. 16, No. 5, 1976, pp. 344–352.

[34] Naik, D. L. and Fronk, T. H., "Effective properties of cell wall layers in bast fiber," *Computational Materials Science*, Vol. 79, 2013, pp. 309 – 315.

[35] Hill, R., "The Elastic Behaviour of a Crystalline Aggregate," *Proceedings of the Physical Society. Section A*, Vol. 65, No. 5, 1952, pp. 349.

[36] Liu, B., Feng, X., and Zhang, S.-M., "The effective Youngs modulus of composites beyond the Voigt estimation due to the Poisson effect," *Composites Science and Technology*, Vol. 69, No. 13, 2009, pp. 2198 – 2204, Smart Composites and Nanocomposites Special Issue with Regular Papaers.

[37] Liu, B., Zhang, L., and Gao, H., "Poisson ratio can play a crucial role in mechanical properties of biocomposites," *Mechanics of Materials*, Vol. 38, No. 12, 2006, pp. 1128 – 1142.

[38] Venkateshwaran, N. and ElayaPerumal, A., "Mechanical and water absorption properties of woven jute/banana hybrid composites," *Fibers and Polymers*, Vol. 13, No. 7, 2012, pp. 907–914.

[39] Gujjala, R., Ojha, S., Acharya, S., and Pal, S., "Mechanical properties of woven jute-glass hybrid-reinforced epoxy composite," *Journal of Composite Materials*, Vol. 48, No. 28, 2014, pp. 3445–3455.

[40] Idicula, M., Joseph, K., and Thomas, S., "Mechanical Performance of Short Banana/Sisal Hybrid Fiber Reinforced Polyester Composites," *Journal of Reinforced Plastics and Composites*, Vol. 29, No. 1, 2010, pp. 12–29.

[41] Flynn, J., Amiri, A., and Ulven, C., "Hybridized carbon and flax fiber composites for tailored performance," *Materials & Design*, Vol. 102, 2016, pp. 21 – 29.

[42] Braga, R. and Jr., P. M., "Analysis of the mechanical and thermal properties of jute and glass fiber as reinforcement epoxy hybrid composites," *Materials Science and Engineering: C*, Vol. 56, 2015, pp. 269 – 273.

APPENDIX

Axis Transformation

To get the elastic properties of any specific fiber, it is necessary to transform the elastic properties of S2 layer from cellulose axis to the fiber axis. For example, The cellulose angle (also known as spiral angle) in flax is 10°. That means cellulose microfibrils are aligned with the fiber axis at an angle of 10°. As the microfibril angle in S2 layer of flax is 10°, one needs to rotate the L and T axes about an axis normal to both of them and normal to the page for 10° and thus get the elastic properties in the fiber axis direction (refer to figure 4.7). The transformation of stiffness matrix of S2 layer can be done like following -

$$D = T_1^{-1}(\alpha) S T_2(\alpha)$$

$$T_1(\alpha) = \begin{pmatrix} m^2 & n^2 & 0 & 0 & 0 & mn \\ n^2 & m^2 & 0 & 0 & 0 & -mn \\ 0 & 0 & 1 & 0 & 0 & 0 \\ 0 & 0 & 0 & m & n & 0 \\ 0 & 0 & 0 & -n & m & 0 \\ -2mn & 2mn & 0 & 0 & 0 & m^2 - n^2 \end{pmatrix}$$

$$T_2(\alpha) = \begin{pmatrix} m^2 & n^2 & 0 & 0 & 0 & 2mn \\ n^2 & m^2 & 0 & 0 & 0 & -2mn \\ 0 & 0 & 1 & 0 & 0 & 0 \\ 0 & 0 & 0 & m & n & 0 \\ 0 & 0 & 0 & -n & m & 0 \\ -mn & mn & 0 & 0 & 0 & m^2 - n^2 \end{pmatrix}$$

where,

$m = cos(\alpha)$

$n = sin(\alpha)$

$\alpha =$ angle of rotaion

T_1 & $T_2 =$ Transformation matrices

$S =$ Compliance matrix before axis rotation

$D =$ Compliance matrix after axis rotation

$\sigma = [\sigma_1\ \sigma_2\ \sigma_3\ \sigma_{23}\ \sigma_{13}\ \sigma_{12}]$

$\epsilon = [\epsilon_1\ \epsilon_2\ \epsilon_3\ \epsilon_{23}\ \epsilon_{13}\ \epsilon_{12}]$